Chiral-odd generalized parton distributions in the large-N_c limit of QCD: Spin-flavor structure, polynomiality, and sum rules

June-Young Kim [*] and Christian Weiss [†]

Theory Center, Jefferson Lab, Newport News, Virginia 23606, USA

(Received 10 December 2024; accepted 12 March 2025; published 9 April 2025)

We study the nonperturbative properties of the nucleon's chiral-odd generalized parton distributions (transversity GPDs) in the large-N_c limit of QCD. This includes the parametric ordering of the spin-flavor components, the polynomiality property of the moments, and the sum rules connecting the GPDs with the tensor form factors. A multipole expansion in the transverse momentum transfer is used to enumerate and interpret the structures in the nucleon matrix element of the chiral-odd partonic operator, including monopole, dipole and quadrupole terms. The $1/N_c$ expansion of the GPDs is performed using the abstract mean-field picture of baryons in the large-N_c limit and its symmetries. We derive a large-N_c relation between the flavor-nonsinglet GPDs E_T^{u-d} and $\tilde{H}_T^{u-d}$ and test it with recent lattice QCD results. We show that the polynomiality property and sum rules of the GPDs are fulfilled with the restricted realization of translational and rotational invariance in the mean-field picture. The results provide a basis for the phenomenological analysis of chiral-odd GPDs and hard exclusive processes in the large-N_c limit, and for calculations in specific dynamical models.

DOI: 10.1103/PhysRevD.111.074007

I. INTRODUCTION

Generalized parton distributions (GPDs) are an essential instrument for expressing nucleon structure in QCD. They describe the nonforward nucleon matrix elements of partonic QCD operators representing correlation functions of the quark and gluon fields at lightlike distances. The GPDs unify the concepts of the nucleon parton densities and elastic form factors (FFs) and open new possibilities of characterizing the dynamical system; see Refs. [1–4] for a review. The transverse coordinate representation of the GPDs describes the spatial distribution of quarks/antiquarks/gluons in the nucleon and allows one to represent it as an extended object in space [5–7]. The moments of the GPDs (x-weighted integrals) describe nucleon FFs of local QCD operators of twist 2 and spin $n \geq 1$, which arise from the expansion of the partonic operator in powers of the lightlike distance. These local operators contain the QCD energy-momentum tensor ($n = 2$), whose FFs describe the distribution of mass, angular momentum, and forces in the nucleon and allow one to quantify its internal mechanical properties [8–11].

[*] Contact author: jykim@jlab.org
[†] Contact author: weiss@jlab.org

The quark GPDs come in two types, determined by the chiral properties of the partonic operator $\bar{\psi}(-z/2)\Gamma\psi(z/2)$, where ψ and $\bar{\psi}$ are the QCD quark fields, z is the lightlike 4-vector distance, $z^2 = 0$, and Γ is a bispinor matrix. The chiral-even operators with $\Gamma = \gamma^+$ or $\gamma^+\gamma^5$ define the so-called chiral-even GPDs. They reduce to the unpolarized and helicity-polarized quark densities in the forward limit, and their first moments are the FFs of the vector and axial vector current. The chiral-odd operators with $\Gamma = \sigma^{+\perp}$ define the chiral-odd GPDs. They correspond to the transversity-polarized quark densities in forward limit, and their first moments are related to the FFs of the local tensor operator $\bar{\psi}(0)\sigma^{\mu\nu}\psi(0)$, which include the tensor charge FF defining the tensor charge at zero momentum transfer. (Here $+$ and $\perp$ are the light cone 4-vector components along the direction of z; definitions are given below.)

The chiral-even GPDs have been extensively studied regarding their general properties, applications to nucleon structure, and model predictions [1–4]. The chiral-odd GPDs remain relatively unexplored, with many of their basic properties still unknown. The chiral-odd GPDs possess unique features and present new probes of nucleon structure. Chiral-odd quark operators do not mix with gluon operators (they are nonsinglets) and depend only weakly on the renormalization scale, which makes them effective probes of nonperturbative nucleon structure; see Ref. [12] for a review. Comparison of chiral-even and chiral-odd structures reveals relativistic effects in the context of the quark-model picture of the nucleon. The chiral-odd GPDs

describe the effect of transverse quark polarization on the spatial distributions [13,14]. Their moments give access not only to the nucleon tensor charge but also to higher multipoles of the tensor operator, such as the anomalous tensor magnetic moment and the quadrupole moment. Studies of the properties of the chiral-odd GPDs are needed to enable these applications to nucleon structure.

GPDs parametrize the nucleon structure sampled in hard exclusive processes in lepton-nucleon scattering in the context of QCD factorization [1–4]. In the asymptotic regime (energy and momentum transfer $\gg$ hadronic scale) the scattering process takes place on a single quark, whose emission and absorption by the nucleon are described by the GPDs. This makes it possible to extract information on the GPDs from observables in exclusive processes. Chiral-even GPDs appear in the factorization of deeply virtual Compton scattering, $l + N \to l + \gamma + N$, and in the asymptotic twist-2 mechanism of exclusive meson production, $l + N \to l' + M + N$. Chiral-odd GPDs appear in the twist-3 mechanism of pseudoscalar meson production, where they are combined with the chiral-odd meson distribution amplitudes [15–18]. While theoretically subleading, this mechanism produces large amplitudes at energy/momentum transfers $\sim$ few GeV and predicts observables consistent with measurements at JLab 6 GeV [19–24]. This opens the prospect of probing chiral-odd GPDs in pseudoscalar meson production experiments at JLab 12 GeV (see Refs. [25,26] for first results), and at higher energies in the CERN COMPASS experiment [27,28] and the future Electron-Ion Collider [29]. The same chiral-odd mechanism can be applied to the time-reversed process of dilepton production in pion-nucleon scattering, $\pi N \to l^+ l^- + N$, which can be measured at J-PARC [30]. Chiral-odd GPDs are also probed in exclusive high-mass pair production processes [31–33]. Quantitative predictions for chiral-odd GPDs are needed to analyze the data and simulate future experiments.

The $1/N_c$ expansion is a powerful method for analyzing nucleon structure in QCD. The limit of a large number of colors corresponds to a semiclassical limit of QCD, in which the dynamics simplifies in characteristic ways yet retains essential nonperturbative features such as the dynamical breaking of conformal and chiral symmetry [34–36]. The N_c scaling of hadron masses, couplings, and FFs can be established on general grounds. Baryons appear as mean-field solutions with mass $\mathcal{O}(N_c)$ and size $\mathcal{O}(N_c^0)$, analogous to solitons in classical field theories [35]. The mean field couples spatial and flavor degrees of freedom and imposes a characteristic spin-flavor symmetry on baryon properties [37,38]. Baryon states with spin-isospin quantum numbers arise from quantization of the rotational zero modes, with the N and Δ appearing as rotational states with $S = T = 1/2$ and $3/2$ [35]. Matrix elements of QCD operators such as GPDs can be analyzed according to their N_c scaling. The different spin-isospin components of the matrix elements exhibit different N_c scaling, dictated by the symmetries of the mean field and the quantization of the zero modes.

Large-N_c methods can be applied to the analysis of nucleon matrix elements of QCD operators at two levels. (i) Deriving the N_c scaling of the spin-flavor components of the matrix elements and relations between them: This can be done using only the symmetries of the mean-field and zero mode quantization. It does not require dynamical input, and the results are model independent. (ii) Making quantitative predictions for matrix elements: This is possible with dynamical models that generate a specific mean-field solution and predict the expectation value of the QCD operator in the mean field. The zero-mode quantization then generates quantitative predictions for the spin-flavor components of matrix elements. An example is the chiral quark-soliton model based on the effective dynamics of massive quarks coupled to a chiral meson field [39–41].

In this work we study the chiral-odd GPDs of the nucleon in the large-N_c limit of QCD. The investigation is divided in two parts. In the first part (reported in the present article) we derive the general properties of the chiral-odd GPDs in large-N_c limit, including the multipole expansion, the N_c scaling of spin-flavor components, the realization of polynomiality, and the sum rules and connection with the tensor FFs. Here we use only model-independent features of baryon structure in the large-N_c limit. In the second part (reported in a subsequent article) we obtain numerical estimates in the chiral quark-soliton model and discuss the dynamical properties of the chiral-odd GPDs, such as the magnitude of the spin-flavor components, valence and sea quark distributions, and the role of long-distance chiral dynamics.

A general technique for performing the $1/N_c$ expansion of GPDs was described in Ref. [1] and applied to the analysis of chiral-even GPDs. Applications to chiral-odd GPDs were considered in Ref. [42]. The present work extends the treatment of the chiral-odd GPDs in several aspects and revises some of the earlier results. New elements are as follows.

Multipole expansion: We systematically employ the multipole expansion to characterize the momentum transfer and spin dependence of the nonforward matrix elements. The method allows us to classify the structures and explain the observed dependence. The use of multipoles is natural in the context of the $1/N_c$ expansion of baryon matrix elements, as the N_c scaling of structures is determined by t-channel spin-isospin quantum numbers (so-called $I = J$ rule) [43–45]. In GPDs the multipole expansion is performed as an expansion in the transverse momentum transfer for fixed longitudinal momentum variables. We compare this two-dimensional (2D) multipole expansion with the three-dimensional (3D) multipole expansion in the Breit frame to explain the observed structures.

Partonic and local operators: We consider in parallel the matrix elements of the chiral-odd partonic operator and the local tensor operator ($n = 1$ moment). The multipole expansion and $1/N_c$ expansion are performed for both operators. This approach helps us to motivate the structures appearing in the multipole expansion of the partonic operator and explain their N_c scaling. We find that the decomposition of the partonic operator includes a quadrupole structure that was omitted in the analysis of Ref. [42]. With the complete decomposition, we are able to derive the N_c scaling of all the spin-flavor components and obtain a new nontrivial large-N_c relation between the leading chiral-odd GPDs E_T^{u-d} and $\tilde{H}_T^{u-d}$, which can be tested with model predictions or experimental data.

Polynomiality in the large-N_c limit: GPD moments are matrix elements of local spin-n tensor operators, whose dependence on the momentum transfer is constrained by relativistic covariance. When expressed in partonic variables, this leads to the so-called polynomiality property, that the GPD moments of spin n are polynomials in the fractional light cone momentum transfer ξ (so-called skewness) of degree not exceeding n [1–4]. It represents a general constraint on the GPDs as functions of the partonic variables and plays an important role in their analysis. In the large-N_c limit the realization of polynomiality is nontrivial, as relativistic covariance is realized only order by order in the $1/N_c$ expansion. This is connected with the fact that the baryon mean field at large N_c breaks translational and rotational invariance, and that they are restored by quantization of the zero modes. The problem of "symmetry breaking by the mean field" is well known from nonrelativistic nuclear physics and has been studied in that context; see Ref. [46] for a review. Polynomiality of the GPDs in the large-N_c limit was demonstrated in the chiral-even sector in Ref. [47], using the chiral quark-soliton model as a specific realization. We show here that polynomiality in the large-N_c limit is also realized in the chiral-odd sector. We present a more general formulation using an abstract mean-field picture and identify what symmetries and other properties of the mean field bring about polynomiality. This approach can help to generalize the large-N_c analysis of GPDs and enable a formulation using group-theoretical methods.

Lattice QCD calculations of chiral-odd GPDs have been performed using local operators (moments) [48–50] and recently developed methods based on high-momentum Euclidean correlation functions [51,52]. The results can be used to test the large-N_c relations for the spin-flavor components of the FFs and GPDs. The $1/N_c$ expansion can explain the hierarchy of structures observed in lattice calculations and use lattice results to predict unknown spin-flavor components.

Section II presents the definition of the chiral-odd GPDs and their general properties. Section III discusses the multipole expansion of the chiral-odd GPDs and the local tensor operator. Section IV analyzes the spin-flavor structure of the chiral-odd GPDs at large N_c. The general method for the $1/N_c$ expansion of GPDs is presented, using the abstract mean-field picture of baryons in the large-N_c limit. The method is then applied to the $1/N_c$ expansion of the chiral-odd GPDs. The N_c scaling of the spin-flavor components and the large-N_c relation between the leading chiral-odd GPDs are derived. The large-N_c relation is then tested with recent lattice QCD results. Section V covers the realization of polynomiality of chiral-odd GPDs at large N_c. The GPDs are represented in a first-quantized form within the abstract mean-field picture, and polynomiality is demonstrated using general properties of the quark single-particle operators. Section VI establishes the connection between the chiral-odd GPDs and the FFs of the local tensor operator in the large-N_c limit. The $1/N_c$ expansion of the FFs is performed, and the realization of the sum rules in the mean-field picture is discussed. Section VII summarizes the conclusions and suggestions for further studies. Appendix A presents the proof of polynomiality of the higher multipoles of the chiral-odd GPDs. Appendix B presents the proof of the sum rules for the higher multipoles of the chiral-odd GPDs and tensor FFs.

II. CHIRAL-ODD GPDs

The matrix element of the chiral-odd partonic QCD operator between nucleon states is defined as

$$\begin{aligned}&\mathcal{M}_{\mathrm{GPDs}}[i\sigma^{+j}]\\&= P^+ \int \frac{dz^-}{2\pi} e^{ixP^+z^-}\\&\quad\times \langle p',s'|\bar{\psi}\left(-\frac{z}{2}\right)\left[-\frac{z}{2},\frac{z}{2}\right] i\sigma^{+j}\psi\left(\frac{z}{2}\right)|p,s\rangle\Big|_{z^+,z_\perp=0}.\end{aligned} \tag{1}$$

ψ and $\bar{\psi}$ are the quark fields, $\sigma^{\mu\nu} \equiv (i/2)[\gamma^\mu,\gamma^\nu]$, and the light cone 4-vector components are $v^\pm \equiv (v^0 \pm v^3)/\sqrt{2}$ and $v_\perp = (v^1, v^2)$. The space-time separation z of the fields is lightlike, and $[-z/2, z/2]$ denotes the gauge link (Wilson line) along the straight lightlike line connecting the points. The initial and final nucleon 4-momenta are p and p', and $P \equiv (p' + p)/2$ is the average 4-momentum. The matrix element Eq. (1) is parametrized as

$$\begin{aligned}\mathcal{M}_{\mathrm{GPDs}}[i\sigma^{+j}] = \bar{u}'\Bigg[&i\sigma^{+j}H_T + \frac{P^+\Delta^j - \Delta^+P^j}{M_N^2}\tilde{H}_T\\&+\frac{\gamma^+\Delta^j - \Delta^+\gamma^j}{2M_N}E_T + \frac{\gamma^+P^j - P^+\gamma^j}{M_N}\tilde{E}_T\Bigg]u.\end{aligned} \tag{2}$$

$u \equiv u(p,s)$ and $\bar{u}' \equiv \bar{u}(p',s')$ are the bispinor wave functions of initial and final nucleon, normalized as $\bar{u}u = \bar{u}'u' = 2M_N$, where M_N is the nucleon mass. s and

s' are the spin quantum numbers; the choice of spin states will be specified in following. $\Delta \equiv p' - p$ is the 4-momentum transfer. The functions H_T, $\tilde{H}_T$, E_T, and $\tilde{E}_T$ are the chiral-odd GPDs. They depend on the partonic variable x, the fractional light cone momentum transfer between the nucleon states, $\xi \equiv -\Delta^+/2P^+$ (skewness); and the invariant momentum transfer $t \equiv \Delta^2$. The GPDs also depend on the renormalization scale of the QCD operator; this dependence will not be indicated explicitly. The four terms in Eq. (2) represent independent covariant structures; their interpretation will be discussed in following.

The QCD operator in Eq. (1) and the GPDs in Eq. (2) depend on the quark flavor $f = (u, d)$. In the following we consider flavor distributions as well as isoscalar/isovector combinations $u \pm d$. The dependence on the quark flavor and nucleon isospin will be indicated as needed.

Because of time reversal invariance the GPDs have definite parity under the transformation $\xi \to -\xi$,

$$F(x, \xi, t) = +F(x, -\xi, t) \quad \text{for } F = H_T, \tilde{H}_T, E_T, \tag{3a}$$

$$F(x, \xi, t) = -F(x, -\xi, t) \quad \text{for } F = \tilde{E}_T. \tag{3b}$$

The partonic operator in Eq. (1) can be expanded in powers of the lightlike separation, generating a series of local operators of increasing spin. The local operator of spin m can be expressed as the x^{m-1}-weighted integral of the nonlocal operator over x (so-called m-th moment),

$$\begin{aligned}&(P^+)^m \int dx x^{m-1} \int \frac{dz^-}{2\pi} e^{ixP^+z^-} \\ &\times \bar{\psi}\left(-\frac{z}{2}\right)\left[-\frac{z}{2}, \frac{z}{2}\right] i\sigma^{+j}\psi\left(\frac{z}{2}\right)\Big|_{z^+, z_\perp = 0} \\ &= \bar{\psi}(0)(i\overleftrightarrow{D}^+)^{m-1} i\sigma^{+j}\psi(0),\end{aligned} \tag{4}$$

where $\overleftrightarrow{D}^\mu = (\vec{D}^\mu - \overleftarrow{D}^\mu)/2$ is the QCD covariant derivative. Using this operator relation it can be shown that the moments of the GPDs are polynomials in ξ [53],

$$\int_{-1}^{1} dx x^{m-1} H_T(x, \xi, t) = \sum_{\substack{i=0 \\ \text{even}}}^{m-1} (-2\xi)^i A_{Tm,i}(t), \tag{5a}$$

$$\int_{-1}^{1} dx x^{m-1} \tilde{H}_T(x, \xi, t) = \sum_{\substack{i=0 \\ \text{even}}}^{m-1} (-2\xi)^i \tilde{A}_{Tm,i}(t), \tag{5b}$$

$$\int_{-1}^{1} dx x^{m-1} E_T(x, \xi, t) = \sum_{\substack{i=0 \\ \text{even}}}^{m-1} (-2\xi)^i B_{Tm,i}(t), \tag{5c}$$

$$\int_{-1}^{1} dx x^{m-1} \tilde{E}_T(x, \xi, t) = \sum_{\substack{i=0 \\ \text{odd}}}^{m-1} (-2\xi)^i \tilde{B}_{Tm,i}(t). \tag{5d}$$

The polynomials are even or odd in ξ according to Eq. (3). The degree of the polynomials representing the m-th moment is $\leq m-1$, with the exact degree depending on the even/oddness of $m-1$ and on the GPD. The coefficients of the polynomials depend only on t and are called the generalized tensor FFs. The polynomiality property Eq. (5) plays a fundamental role in the structure of the GPDs.

The first moments of the chiral-odd GPDs are connected with the nucleon tensor FFs. The nucleon matrix element of the local tensor operator is parametrized as

$$\begin{aligned}\mathcal{M}_{\text{FFs}}[i\sigma^{\mu\nu}] &= \langle p', s'|\bar{\psi}(0) i\sigma^{\mu\nu}\psi(0)|p, s\rangle \\ &= \bar{u}'\left[i\sigma^{\mu\nu} H_T(t) + \frac{P^\mu\Delta^\nu - \Delta^\mu P^\nu}{M_N^2}\tilde{H}_T(t)\right. \\ &\quad \left. + \frac{\gamma^\mu\Delta^\nu - \Delta^\mu\gamma^\nu}{2M_N} E_T(t)\right] u.\end{aligned} \tag{6}$$

Here the tensor decomposition is covariant and does not reference the light cone direction. We denote the tensor FFs in Eq. (6) by the same symbols as the GPDs, to emphasize the correspondence of the structures; the functions can be distinguished by their arguments. Comparing Eqs. (1) and (6), one has

$$\int_{-1}^{1} dx H_T(x, \xi, t) = A_{T10}(t) \equiv H_T(t), \tag{7a}$$

$$\int_{-1}^{1} dx \tilde{H}_T(x, \xi, t) = \tilde{A}_{T10}(t) \equiv \tilde{H}_T(t), \tag{7b}$$

$$\int_{-1}^{1} dx E_T(x, \xi, t) = B_{T10}(t) \equiv E_T(t), \tag{7c}$$

$$\int_{-1}^{1} dx \tilde{E}_T(x, \xi, t) = 0. \tag{7d}$$

The vanishing first moment of $\tilde{E}_T$ is due to its antisymmetry in ξ.

In the forward limit, $\xi \to 0$ and $|t| \to 0$, the chiral-odd GPD H_T reduces to the transversity parton distribution function

$$H_T(x, \xi = 0, t = 0) = h_1(x). \tag{8}$$

Its first moment is known as the nucleon's tensor charge

$$\int_{-1}^{1} dx H_T(x, \xi = 0, t = 0) = \int_{-1}^{1} dx h_1(x) = H_T(0) = g_T. \tag{9}$$

In applications to exclusive pseudoscalar meson production processes one introduces the linear combination of GPDs,

$$\bar{E}_T \equiv E_T + 2\tilde{H}_T. \tag{10}$$

Its first moment in the forward limit is known as the nucleon's anomalous tensor magnetic moment,

$$\int_{-1}^{1} dx \bar{E}_T(x,\xi=0,t=0) = E_T(0) + 2\tilde{H}_T(0) = \kappa_T. \quad (11)$$

Thus the chiral-odd GPDs provide information on fundamental characteristics of the nucleon derived from the local tensor operator.

III. MULTIPOLE EXPANSION

A. Multipole expansion of chiral-odd GPDs

To analyze the structure of the chiral-odd GPDs and FFs, it is useful to perform a multipole expansion of the matrix elements of the chiral-odd operators. The multipoles allow one to enumerate the independent structures in the matrix element and exhibit their spin and orbital angular momentum content. The multipole expansion prepares the matrix element for the $1/N_c$ expansion, where the multipoles have definite N_c scaling, determined by their spin and isopspin quantum numbers.

We consider here the multipole expansion of both GPDs (nonlocal partonic operator) and FFs (local operator). The multipole expansion of the GPDs is performed in light-front variables, as an expansion in the 2D transverse momentum transfer $\boldsymbol{\Delta}_\perp$, constrained by 2D rotational invariance (conservation of angular momentum along the 3-direction, called longitudinal angular momentum). The multipole expansion of the FFs can be performed either as an expansion in the 2D light-front momentum transfer, in same way as for the GPDs, or as an expansion in the 3D momentum transfer $\boldsymbol{\Delta}$ in the Breit frame, constrained by 3D rotational invariance (conservation of all components of the angular momentum). Comparison of the two expansions provides insight into the origin of the 2D light-front structures and implements the constraints on the light-front multipoles arising from 3D rotational invariance (so-called angular conditions) and discrete symmetries.

The multipole expansion of the matrix element of the chiral-odd partonic operator is performed using light-front momentum variables for the nucleon states. We consider the parametrization, Eq. (2), in a class of reference frames where the average nucleon 4-momentum has zero transverse component, $\boldsymbol{P}_\perp = 0$, and the momentum transfer has nonzero component $\boldsymbol{\Delta}_\perp \neq 0$. In these frames the light-front 4-vector components of P and Δ are given by (in the notation $v = [v^+, v^-, \boldsymbol{v}_\perp]$)

$$P = \left[P^+, \frac{M_N^2 + |\boldsymbol{\Delta}_\perp|^2/4}{2P^+(1-\xi^2)}, \boldsymbol{0}_\perp\right], \quad (12a)$$

$$\Delta = \left[-2\xi P^+, \frac{\xi(M_N^2 + |\boldsymbol{\Delta}_\perp|^2/4)}{P^+(1-\xi^2)}, \boldsymbol{\Delta}_\perp\right]. \quad (12b)$$

The mass shell conditions of the initial and final nucleon 4-momenta imply that

$$\Delta \cdot P = 0, \qquad P^2 + \frac{\Delta^2}{4} = M_N^2. \quad (13)$$

The condition $\boldsymbol{P}_\perp = 0$ does not determine a unique frame but an equivalence class of frames related by longitudinal boosts; the value of P^+ remains arbitrary and specifies a particular frame in the class. The nucleon spin states are chosen as light-front helicity states, prepared from rest-frame spin states by a sequence of light-front boosts [54]. Explicit expressions for the light-front bispinors in terms of rest-frame 2-component spinors are given e.g. in Ref. [55].

In the frames of Eq. (12) the only transverse vector characterizing the matrix element is the momentum transfer $\boldsymbol{\Delta}_\perp$. The matrix element can therefore be expanded in 2D multipole structures in $\boldsymbol{\Delta}_\perp$. The 2D rank-$n$ irreducible tensors are defined as [56]

$$X_0 = 1 \quad (L_3 = 0), \quad (14a)$$

$$X_1^i = \boldsymbol{n}_\perp^i \quad (L_3 = \pm 1), \quad (14b)$$

$$X_2^{ij} = \boldsymbol{n}_\perp^i \boldsymbol{n}_\perp^j - \frac{1}{2}\delta^{ij} \quad (L_3 = \pm 2), \quad (14c)$$

where $\boldsymbol{n}_\perp \equiv \boldsymbol{\Delta}_\perp/|\boldsymbol{\Delta}_\perp|$ and $i, j = 1, 2$. The tensors correspond to structures with longitudinal orbital angular momentum $L_3 = 0, \pm 1, \pm 2$, respectively, as indicated in Eq. (14). The orbital structures are accompanied by spin structures formed from the spin wave functions of the initial and final nucleon. The spin structures appear as bilinear forms in the 2-component spinors describing the spin wave function of each nucleon in its rest frame,

$$\chi^\dagger(s')\hat{O}\chi(s). \quad (15)$$

The quantization axis of the spinors can be chosen along any direction in the rest frame; the spin quantum numbers s and s' are then defined as the spin projections along this axis. In the following the quantization axis is chosen as the 3-axis, and the spinors are eigenspinors of the 3-component of the spin operator,

$$\frac{\sigma^3}{2}\chi(S_3) = S_3\chi(S_3), \qquad S_3 = \pm 1/2, \quad (16)$$

and the spin quantum numbers are the spin projections along the 3-axis in the rest frame,[1]

[1]The quantization axis can also be chosen as the transverse 1-axis, by defining the spinors as eigenspinors of $\sigma^1/2$. The transversely polarized spinors are linear combinations of the longitudinally polarized spinors. The subsequent arguments concerning conservation of the longitudinal angular momentum refer to the angular momentum of the bilinear form of Eq. (15) and do not depend on the choice of spin states.

$$s \equiv S_3, \qquad s' \equiv S_3'. \tag{17}$$

The operator $\hat{O}$ in Eq. (15) can be the unit operator 1 or a component of the spin operator $\boldsymbol{S} = \boldsymbol{\sigma}/2$. In the present context the independent structures characterizing the transition are (here $i = 1, 2$)

$$\hat{O} = \mathbf{1} \quad (L_3 = 0), \tag{18a}$$

$$\sigma^3 \quad (L_3 = 0), \tag{18b}$$

$$\sigma^i \quad (L_3 = \pm 1). \tag{18c}$$

These scalar and vector structures have longitudinal angular momentum $L_3 = 0, 0, \pm 1$, respectively, as indicated in Eq. (14). Expanding the matrix element Eq. (2) in the structures of Eqs. (14) and (18), we obtain

$$\mathcal{M}_{\mathrm{GPDs}}[i\sigma^{+j}] = \frac{2P^+}{\sqrt{1-\xi^2}} \left\{ i\epsilon^{3jm}\sigma^m X_0 \left[(1-\xi^2) H_T + \frac{|\boldsymbol{\Delta}_\perp|^2}{4M_N^2} \tilde{H}_T - \xi^2 E_T + \xi \tilde{E}_T \right] + \mathbf{1} X_1^j \frac{|\boldsymbol{\Delta}_\perp|}{2M_N} (2\tilde{H}_T + E_T - \xi \tilde{E}_T) \right.$$
$$\left. + i\epsilon^{3jm}\sigma^3 X_1^m \frac{|\boldsymbol{\Delta}_\perp|}{2M_N} (-\xi E_T + \tilde{E}_T) + i\epsilon^{3ml}\sigma^l X_2^{mj} \frac{|\boldsymbol{\Delta}_\perp|^2}{4M_N^2} (2\tilde{H}_T) \right\}. \tag{19}$$

Here it is implied that the spin operators are contracted with the nucleon rest-frame spinors as in Eq. (15), and that the matrix element is a function of S_3 and S_3'. One sees that the four structures in Eq. (19) contain one orbital monopole, two dipoles, and one quadrupole.

The number of independent structures in Eq. (19) can be explained by the addition of longitudinal angular momentum in the light-front representation. The matrix element of the partonic operator with σ^{+j} is a transverse vector and has components with $L_3 = \pm 1$. The four structures in Eq. (19) are those that can be formed by combining the orbital structures in Eq. (14) and the spin structures in Eq. (18) such that L_3 adds up to ± 1. The parity of the structures involving the spin operators σ^3 and σ^i is adjusted by the 2D pseudotensor ϵ^{3ij}; the existence of this tensor is specific to the light-front representation with the preferred 3-direction.

The multipole expansion of the chiral-odd matrix element Eq. (19) includes a term with the orbital quadrupole X_2. It appears from the coupling of the spin dipole Eq. (18) with the orbital quadrupole Eq. (14). In this way the orbital quadrupole can be present even though nucleon-to-nucleon matrix elements cannot support a spin quadrupole structure. The presence of the orbital quadrupole structure is confirmed by the multipole expansion of the local tensor operator in the Breit frame (see Sec. IV A). It plays an important role in the $1/N_c$ expansion of the chiral-odd GPDs (see Sec. IV). The quadrupole structure was not included in the analysis of Ref. [42].

The quadrupole structure appears only in the chiral-odd, not in the chiral-even GPDs. In the chiral-even GPDs the operators γ^+ and $\gamma^+\gamma_5$ have $L_3 = 0$. In this case the addition of longitudinal angular momentum produces four independent structures formed from the $L_3 = 0$ and ± 1 structures in Eqs. (14) and (18), but cannot involve the $L_3 = 2$ orbital structure. This causes an essential difference between the nonforward matrix elements of the chiral-odd and chiral-even operators, which is not apparent from the forward limit.

The combinations of GPDs appearing in Eq. (19) can be referred to as the "multipole GPDs." They represent an alternative definition of the chiral-odd GPDs with an obvious physical interpretation and appear naturally in the $1/N_c$ expansion (see Sec. IV). Their physical properties and connection with observables could be explored also independently of the $1/N_c$ expansion.

B. Multipole expansion of tensor FFs

The multipole expansion of the matrix element of the local tensor operator can be performed in light-front momentum variables, in the same way as for the nonlocal partonic operator. We consider the matrix element Eq. (6) in the class of frames defined by Eq. (12) with $\xi = 0$, where the 4-vector components are

$$P = \left[P^+, \frac{M_N^2 + |\boldsymbol{\Delta}_\perp|^2/4}{2P^+}, \mathbf{0}_\perp \right], \tag{20a}$$

$$\Delta = [0, 0, \boldsymbol{\Delta}_\perp], \tag{20b}$$

and where

$$t = -|\boldsymbol{\Delta}_\perp|^2. \tag{21}$$

These are the so-called Drell-Yan-West frames used in the analysis of FFs in light-front quantization [54]. In these frames the matrix element can be expanded in the 2D multipoles in $\boldsymbol{\Delta}_\perp$. The result for the local tensor operator can be obtained by setting $\xi = 0$ in Eq. (19) and using the relations Eq. (7) between the moments of the GPDs and the tensor FFs. We obtain

$$\mathcal{M}_{\mathrm{FFs}}[i\sigma^{+j}] = 2P^+\left[i\epsilon^{3jm}\sigma^m X_0\left(H_T - \frac{t}{4M_N^2}\tilde{H}_T\right) + \mathbf{1}X_1^j\frac{\sqrt{-t}}{2M_N}(2\tilde{H}_T + E_T) + i\,\epsilon^{3jl}\sigma^m X_2^{lm}\frac{t}{4M_N^2}(2\tilde{H}_T)\right], \tag{22}$$

where we have set $|\boldsymbol{\Delta}_\perp| = \sqrt{-t}$. One sees that the local tensor operator generates only three structures. The absence of the orbital dipole structure $i\epsilon^{3jm}X_1^m\sigma^3$ compared to the nonlocal partonic operator Eq. (19) is due to time reversal invariance, which causes the vanishing of the first moment of the GPD $\tilde{E}_T$; see Eq. (7). The 2D multipole expansion of the local operator is thus constrained by considerations beyond longitudinal angular momentum conservation.

The multipole expansion of the local tensor operator can also be performed using the 3D vector components, preserving 3D rotational invariance. We consider the matrix element in the Breit frame, where the average nucleon 3-momentum is zero, $\boldsymbol{P} = 0$, and where the 4-momentum components are given by [in the notation $v = (v^0, \boldsymbol{v})$]

$$P = (\bar{M}, \mathbf{0}), \qquad \Delta = (0, \boldsymbol{\Delta}), \tag{23}$$

with

$$|\boldsymbol{\Delta}|^2 = -t, \qquad \bar{M} \equiv \sqrt{M_N^2 - t/4}. \tag{24}$$

The nucleon spin states are now chosen as canonical spin states, obtained by canonical boosts from the rest-frame spin states. In this setup the matrix elements of tensor operators are constrained by 3D angular momentum conservation. The 3D rank-n irreducible tensors are defined as

$$Y_0 = 1 \quad (L = 0), \tag{25a}$$

$$Y_1^i = \boldsymbol{n}^i \quad (L = 1), \tag{25b}$$

$$Y_2^{ij} = \boldsymbol{n}^i\boldsymbol{n}^j - \frac{1}{3}\delta^{ij} \quad (L = 2), \tag{25c}$$

where $\boldsymbol{n} \equiv \boldsymbol{\Delta}/|\boldsymbol{\Delta}|$; $i,\ j = 1,\ 2,\ 3$; and where we have indicated the orbital angular momentum of the structures. The spin operators appearing in the 3D expansion are

$$\mathbf{1}, \qquad L = 0, \tag{26a}$$

$$\sigma^i, \qquad L = 1. \tag{26b}$$

The expansion of the matrix element Eq. (6) is now performed separately for the $0j$ and ij components ($i,\ j = 1,\ 2,\ 3$). We obtain

$$\mathcal{M}_{\mathrm{FFs}}[i\sigma^{0j}] = 2M_N\left\{\mathbf{1}Y_1^j\frac{\sqrt{-t}}{2M_N}\left[H_T + \frac{2\bar{M}^2}{M_N^2}\tilde{H}_T + E_T\right]\right\}, \tag{27a}$$

$$\mathcal{M}_{\mathrm{FFs}}[i\sigma^{ij}] = 2M_N\left\{i\epsilon^{ijk}\sigma^k Y_0\left[\frac{1}{3}\left(\frac{\bar{M}}{M_N} + 2\right)H_T + \frac{t}{6M_N^2}E_T\right] + i\epsilon^{ijk}\sigma^m Y_2^{km}\left[\left(\frac{\bar{M}}{M_N} - 1\right)H_T - \frac{t}{4M_N^2}E_T\right]\right\}. \tag{27b}$$

The multipole structures are now constrained by angular momentum conservation following from 3D rotational invariance. They are also constrained by the discrete symmetries of parity and time reversal, which act on the 3D vectors in a simple manner. Note that the orbital quadrupole structure Y_2 is present in the 3D expansion.

The 2D and 3D multipole expansions can be compared directly, in a way that the structures appearing in both expansions can be matched with each other. This is done by going to the special light-front frame that is identical to the Breit frame [57], namely the frame of Eq. (20) with $P^+ = \bar{M}/\sqrt{2}$, where

$$P^+ = P^- = \frac{\bar{M}}{\sqrt{2}}, \qquad P^0 = \frac{1}{\sqrt{2}}(P^+ - P^-) = \bar{M}. \tag{28}$$

In this frame both expansions are valid, and the expressions can be equated. The 2D light-front components are obtained as the linear combination of the 3D components,

$$\sigma^{+j} = \frac{1}{\sqrt{2}}(\sigma^{0j} + \sigma^{3j}). \tag{29}$$

Comparing the expansions Eqs. (22) and (27) in this way, we observe the following:

(i) The 2D multipole structure Eq. (22) is induced by the 3D multipole structure Eq. (27) as follows:

$$i\epsilon^{ijk}\sigma^k Y_0 \to i\epsilon^{3jk}\sigma^k X_0, \tag{30a}$$

$$\mathbf{1}Y_1^j \to \mathbf{1}X_1^j, \tag{30b}$$

$$i\epsilon^{ijk}\sigma^m Y_2^{km} \to i\epsilon^{3jk}\sigma^m X_2^{km},\ i\epsilon^{3jk}\sigma^k X_0. \tag{30c}$$

The 3D monopoles and dipoles reduce directly to their 2D counterparts. The 3D quadrupole reduces to a 2D quadrupole and a 2D monopole. Such behavior is expected, as the 2D projection of a 3D traceless tensor can be a 2D traceless or traceful tensor. This phenomenon has been investigated in the context of Abel tomography for spin-1 particles [58]. It shows that the 3D quadrupole structure in the tensor matrix

element affects not only the results for the 2D quadrupole but also the monopole.

(ii) The t-dependent functions accompanying the multipoles in the 2D and 3D expansions show differences at the level of terms $\propto \sqrt{-t}/M_N$. They are due to the fact that the 2D expansion was performed using light-front helicity states, while the 3D expansion was performed using canonical spin states. This effect has been discussed in connection with charge and current densities in hadrons and is well understood [59]. It could be corrected by performing the spin rotation transforming the canonical into light-front bispinors (Melosh rotation) in the 3D expression before matching with the 2D expression. In the large-N_c limit the effect of the spin rotation is suppressed by $1/N_c$ and can be neglected when computing the multipole FFs in leading order.

IV. SPIN-FLAVOR STRUCTURE AT LARGE N_c

A. $1/N_c$ expansion in mean-field picture

The $1/N_c$ expansion of nucleon matrix elements of QCD composite operators (local or partonic) can be performed using a method based on the mean-field picture of baryons in the large-N_c limit. Baryons are characterized by a mean field with contracted spin-flavor symmetry, from which spin-isospin states emerge through quantization of the zero modes. The QCD operators are first evaluated in the mean field, which imposes the spin-flavor symmetry on the expectation value; the transition matrix elements between spin-isospin are then obtained from the quantization of the zero modes. The method uses only abstract features of the mean-field picture (symmetries, parametric scaling) and does not refer to any specific dynamics. The results for the N_c scaling of nucleon matrix elements are model independent and equivalent to those obtained with group-theoretical approaches [38]. The mean-field method of the $1/N_c$ expansion is particularly convenient for partonic operators and has been used extensively in the analysis of GPDs [1].

In the large-N_c limit baryon states are classified by the emergent spin-flavor symmetry. The N and Δ appear in the representation with spin-isospin $S = T = 1/2$ and $3/2$. The baryon states are characterized by their spin-isospin quantum numbers $B \equiv \{S = T, S_3, T_3\}$. The baryon masses are $M_{N,\Delta} = \mathcal{O}(N_c)$, and the splitting is $M_N - M_\Delta = \mathcal{O}(N_c^{-1})$. The $1/N_c$ expansion of baryon matrix elements is performed in a class of frames where the initial and final baryons have 3-momenta and energies of the order

$$|\boldsymbol{p}|, |\boldsymbol{p}'| = \mathcal{O}(N_c^0), \tag{31a}$$

$$p^0, p'^0 = M_N + \mathcal{O}(1/N_c) = \mathcal{O}(N_c). \tag{31b}$$

The baryon states are normalized as

$$\langle \boldsymbol{p}', B' | \boldsymbol{p}, B \rangle = 2p^0 (2\pi)^3 \delta^{(3)}(\boldsymbol{p}' - \boldsymbol{p}) \delta_{B'B},$$
$$\delta_{B'B} \equiv \delta_{S'S} \delta_{S_3' S_3} \delta_{T'T} \delta_{T_3' T_3}. \tag{32}$$

In this study we consider $N \to N$ matrix elements; the following discussion can easily be extended to $N \to \Delta$ matrix elements.

One considers the matrix element of a partonic QCD operator of the form

$$\langle \boldsymbol{p}', B' | \bar{\psi}_{\alpha' f'}(-z/2) [-z/2, z/2] \psi_{\alpha f}(z/2) | \boldsymbol{p}, B \rangle, \tag{33}$$

where $z = (z^0, \boldsymbol{z})$ is the lightlike separation of the fields, $z^2 = (z^0)^2 - |\boldsymbol{z}|^2 = 0$. Summation over color indices is implied; $[-z/2, z/2]$ is the gauge link along the straight line connecting the points $-z/2$ and $z/2$. It will be omitted in the following expressions for brevity but is always assumed to be present. α and α' are the bispinor indices of the fields; it is assumed that the matrix element Eq. (33) will be contracted with an external bispinor matrix,

$$\Gamma_{\alpha'\alpha} \langle .. | \bar{\psi}_{\alpha' f'} \psi_{\alpha f} | .. \rangle = \langle .. | \bar{\psi}_{f'} \Gamma \psi_f | .. \rangle. \tag{34}$$

f and f' are the flavor indices; we assume two light flavors (u, d) and exact isospin symmetry. The $1/N_c$ expansion of the matrix element Eq. (33) is performed as follows.

In the first step one takes the expectation value of the operator in the mean-field state of the large-N_c baryon, with the mean field centered at the origin,

$$\langle \mathrm{mf} | \bar{\psi}_{\alpha' f'}(y - z/2) \psi_{\alpha f}(y + z/2) | \mathrm{mf} \rangle = \mathcal{F}_{\alpha' f', \alpha f}(z^0, \boldsymbol{z} | \boldsymbol{y}). \tag{35}$$

Here $y = (y^0, \boldsymbol{y})$ is the center coordinate of the partonic operator; the displacement from the center of the mean field is necessary to account for the momentum transfer to the baryon (see below). The expectation value Eq. (35) defines a function of the space-time coordinates and spinor/flavor indices of the operator. This function is regarded as an abstract object (or parametrization): its specific form is governed by dynamics and can only be determined in models, but its symmetries can be established on general grounds. The mean field is localized in space and breaks translational invariance in space; the expectation value of the operator therefore depends on both coordinates $\boldsymbol{z}$ and $\boldsymbol{y}$. The mean field is time independent (static) and preserves translational invariance in time; the expectation value therefore depends only on the time difference z^0 of the fields, not on the average time y^0.

Most importantly, the mean field possesses the spin-flavor symmetry characteristic of baryons in the large-N_c limit ("hedgehog symmetry") [60]. It implies that the expectation value Eq. (35) is invariant under combined spatial, spin, and flavor rotations of the operator (see Fig. 1),

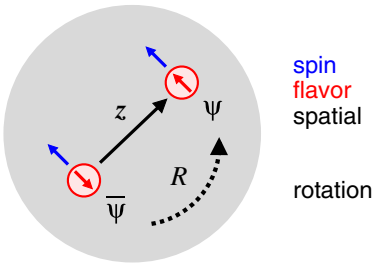

FIG. 1. Visualization of the spin-flavor symmetry of the mean-field expectation value of the partonic operator Eq. (35). The mean-field expectation value is invariant under combined spatial, spin, and flavor rotations of the operator, Eq. (36).

$$S^{-1}_{\beta'\alpha'}S_{\alpha\beta}R^{-1}_{g'f'}R_{fg}\mathcal{F}_{\beta'g',\beta g}(z^0,Oz|Oy)=\mathcal{F}_{\alpha'f',\alpha f}(z^0,z|y). \quad (36)$$

Here R is an $SU(2)$ rotation matrix (applied to the flavor rotations), $O\equiv O(R)$ is the associated $O(3)$ rotation matrix (applied to the spatial rotations),

$$O^{ab}\equiv\frac{1}{2}\mathrm{tr}[R^{-1}\tau^a R\tau^b] \quad (a,b=1,2,3), \quad (37)$$

and $S\equiv S(R)$ is the associated bispinor rotation matrix [61] (applied to the spin rotations). When the bispinor indices are contracted with an external matrix Γ of 3D vector/tensor character as in Eq. (34), the vector/tensor indices on the matrix rotate with the $O(3)$ rotation matrix, Eq. (37). Equation (36) imposes the spin-flavor symmetry of large-N_c baryons on the operator matrix elements and plays a central role in the $1/N_c$ expansion.

In the second step one quantizes the translational zero mode of the mean field and projects on baryon states with definite momenta. In leading order of $1/N_c$ this is done by shifting the center of the mean field to position $\boldsymbol{X}$ and integrating over the collective coordinate with the wave functions $e^{i\boldsymbol{p}\boldsymbol{X}}$ and $e^{-i\boldsymbol{p}'\boldsymbol{X}}$. Because of translational invariance the mean field expectation value depends only on the difference between the center coordinate of the operator and the mean field, $\boldsymbol{y}-\boldsymbol{X}$. The projection can therefore be done equivalently by leaving the mean field centered at $\boldsymbol{X}=0$ and integrating over $\boldsymbol{y}$, with the corresponding change of variables in the wave functions. We define

$$\begin{aligned}&\langle \boldsymbol{p}',\mathrm{mf}|\bar\psi_{\alpha'f'}(-z/2)\psi_{\alpha f}(z/2)|\boldsymbol{p},\mathrm{mf}\rangle\\&\equiv 2M_N\int d^3y e^{i(\boldsymbol{p}'-\boldsymbol{p})\cdot\boldsymbol{y}}\mathcal{F}_{\alpha'f',\alpha f}(z^0,z|y)\\&=2M_N\int d^3y e^{i(\boldsymbol{p}'-\boldsymbol{p})\cdot\boldsymbol{y}}\\&\quad\times\langle\mathrm{mf}|\bar\psi_{\alpha'f'}(-z^0/2,\boldsymbol{y}-\boldsymbol{z}/2)\psi_{\alpha f}(z^0/2,\boldsymbol{y}-\boldsymbol{z}/2)|\mathrm{mf}\rangle.\end{aligned} \quad (38)$$

Equation (38) represents the matrix element of the operator between large-N_c baryon states with definite momenta but as yet indefinite spin-isospin and is referred to as the mean-field matrix element (or soliton matrix element). This "intermediate" object has interesting properties, and several aspects of large-N_c baryon structure can already be discussed at this level (see the application to GPDs in Sec. IV B).

In the third step one quantizes the rotational zero mode of the mean field in position and flavor space and projects on baryon states with the desired spin-isospin quantum numbers. In leading order of $1/N_c$ this is done by integrating over the flavor rotations R, Eq. (36), with rotational wave functions $\phi_B(R)$ and $\phi^*_{B'}(R)$ describing baryon states with spin-isospin quantum numbers B and B' [35,62],

$$\begin{aligned}&\langle \boldsymbol{p}',B'|\bar\psi_{\alpha'f'}(-z/2)\psi_{\alpha f}(z/2)|\boldsymbol{p},B\rangle\\&=\int dR\phi^*_{B'}(R)\phi_B(R)\\&\quad\times R^{-1}_{g'f'}R_{fg}\langle \boldsymbol{p}',\mathrm{mf}|\bar\psi_{\alpha g'}(-z/2)\psi_{\alpha g}(z/2)|\boldsymbol{p},\mathrm{mf}\rangle.\end{aligned} \quad (39)$$

The rotational wave functions are given by the Wigner finite-rotation matrices as [1]

$$\begin{aligned}\phi_B(R)&\equiv\phi^{S=T}_{S_3T_3}(R)\\&=\sqrt{2S+1}(-1)^{T+T_3}D^{S=T}_{-T_3,S_3}(R).\end{aligned} \quad (40)$$

Equations (38) and (39) represent the transition matrix element of the QCD operator in leading nonvanishing order of the $1/N_c$ expansion. The spin-flavor symmetry of the mean field, Eq. (36), restricts the spin-isospin structures emerging from the rotational integral and determines the N_c scaling of the spin-flavor components of the matrix element.

In the analysis here it is assumed that the partonic operator is renormalized at a scale $\mu^2\gg\Lambda^2_{\mathrm{QCD}}$, sufficiently large to allow for perturbative treatment of the scale dependence (evolution). The renormalization scale is subsumed in the definition of the mean-field expectation value Eq. (35) and does not affect the N_c scaling of the spin-flavor components of the matrix element derived from it, which is the object of study here. The value of the renormalization scale becomes relevant only when one attempts to calculate the mean-field expectation value of the operator in models of nonperturbative dynamics.

B. $1/N_c$ expansion of chiral-odd GPDs

In order to set up the $1/N_c$ expansion of the chiral-odd GPDs, one has to specify the parametric order of the kinematic variables in the nonforward matrix element, Eq. (1). The $1/N_c$ expansion is performed with nucleon 3-momenta $\mathcal{O}(N_c^0)$, Eq. (31). This assignment defines a class of frames related by boosts, which includes the frames used in the 2D and 3D multipole expansions (see Sec. III). The average and difference of the initial and final momenta are of the order ($i=1,2,3$)

$$P^i = \mathcal{O}(N_c^0), \qquad P^0 = M_N + \mathcal{O}(N_c^{-1}), \tag{41a}$$

$$\Delta^i = \mathcal{O}(N_c^0), \qquad \Delta^0 = \mathcal{O}(N_c^{-1}), \tag{41b}$$

which implies that the momentum transfer variables in the GPDs are of the order

$$\xi = \mathcal{O}(N_c^{-1}), \qquad |t| = \mathcal{O}(N_c^0). \tag{42}$$

The partonic variable x is taken to be of the order

$$x = \mathcal{O}(N_c^{-1}), \tag{43}$$

which is the standard regime considered in the $1/N_c$ expansion of nucleon parton distributions [63], corresponding to nonexceptional configurations with quark momenta $\mathcal{O}(N_c^0)$ in the nucleon rest frame.

We now perform the $1/N_c$ expansion of the matrix element of the chiral-odd partonic operator, Eq. (1), using the method of Sec. IV A. The mean-field matrix element of the partonic operator between large-N_c baryon states with momenta $\boldsymbol{p}$ and $\boldsymbol{p}'$ is defined according to Eq. (38). This matrix element can be parametrized in the form

$$\begin{aligned}\frac{M_N}{\sqrt{2}}\int\frac{dz^-}{2\pi}\,e^{ixP^+z^-}\langle \boldsymbol{p}', \mathrm{mf}|\bar\psi_{f'}(-z/2)i\sigma^{+j}\psi_f(z/2)|\boldsymbol{p}, \mathrm{mf}\rangle\Big|_{z^+,\boldsymbol{z}_\perp=0} &= \frac{2M_N}{\sqrt{2}}\left[-3i\epsilon^{3jm}(\tau^m)_{f'f}X_0 G_{\mathrm{mf},0} + \mathbf{1}_{f'f}X_1^j\frac{|\boldsymbol{\Delta}_\perp|}{2M_N}G_{\mathrm{mf},1}\right.\\ &\quad - 3i\epsilon^{3jm}(\tau^3)_{f'f}X_1^m\frac{|\boldsymbol{\Delta}_\perp|}{2M_N}\tilde G_{\mathrm{mf},1}\\ &\quad \left. - 3i\epsilon^{3jl}(\tau^m)_{f'f}X_2^{lm}\frac{|\boldsymbol{\Delta}_\perp|^2}{4M_N^2}G_{\mathrm{mf},2}\right].\end{aligned} \tag{44}$$

The decomposition mirrors the multipole expansion of Eq. (19) but takes into account the spin-flavor symmetry of the mean field. The flavor dependence is carried by the isoscalar and isovector structures 1 and τ^a. The terms in Eq. (44) are invariant under combined flavor and spatial rotations, Eq. (36), which includes rotation of the spatial component of the lightlike separation z. The functions

$$G_{\mathrm{mf},0}, G_{\mathrm{mf},1}, \tilde G_{\mathrm{mf},1}, G_{\mathrm{mf},2} = \mathrm{functions}(x,\xi,t) \tag{45}$$

are the mean-field GPDs and depend on the variables x, ξ, and t in the parametric domain of Eqs. (43) and (42). The subscript denotes the multipole order in the momentum transfer $\boldsymbol{\Delta}_\perp$. Note that Eq. (44) contains a term with the quadrupole structure X_2 and a quadrupole mean-field GPD $G_{\mathrm{mf},2}$; this structure was not included in the analysis of Ref. [42].

The projection on spin-isospin states is done by integrating over the flavor rotations of the mean-field matrix element Eq. (44) according to Eq. (39). The rotations of the structures in Eq. (44) are performed as

$$\mathbf{1} \to \mathbf{1}, \qquad \tau^a \to O^{ab}\tau^b, \tag{46}$$

where $O \equiv O(R)$ is the $O(3)$ rotation matrix Eq. (37). We obtain

$$\begin{aligned}\frac{M_N}{\sqrt{2}}\int\frac{dz^-}{2\pi}\,e^{ixP^+z^-}\langle \boldsymbol{p}', B'|\bar\psi_{f'}(-z/2)i\sigma^{+j}\psi_f(z/2)|\boldsymbol{p}, B\rangle\Big|_{z^+,\boldsymbol{z}_\perp=0} &= \frac{2M_N}{\sqrt{2}}\left\{\mathbf{1}_{f'f}\langle 1\rangle_{B'B}\left[X_1^j\frac{|\boldsymbol{\Delta}_\perp|}{2M_N}G_{\mathrm{mf},1}\right]\right.\\ &\quad - 3i\epsilon^{3jl}(\tau^k)_{f'f}\langle O^{km}\rangle_{B'B}\left[\delta^{ml}X_0 G_{\mathrm{mf},0}\right.\\ &\quad \left.\left. + \delta^{m3}X_1^l\frac{|\boldsymbol{\Delta}_\perp|}{2M_N}\tilde G_{\mathrm{mf},1} + X_2^{lm}\frac{|\boldsymbol{\Delta}_\perp|^2}{4M_N^2}G_{\mathrm{mf},2}\right]\right\}.\end{aligned} \tag{47}$$

The integral over rotations with the wave function Eq. (40) is denoted as

$$\langle\ldots\rangle_{B'B} \equiv \int dR\,\phi^{*S'=T'}_{S_3'T_3'}(R)\ldots\phi^{S=T}_{S_3T_3}(R) \tag{48}$$

and evaluates to

$$\langle 1\rangle_{B'B} = \delta_{B'B}, \tag{49a}$$

$$\langle O^{km}\rangle_{B'B} = -\sqrt{\frac{2S+1}{2S'+1}}\langle SS_3, 1b|S'S_3'\rangle \times\langle TT_3, 1a|T'T_3'\rangle U^{\rm SC}_{ak}U^{\rm SC}_{bm}, \tag{49b}$$

where $a, b = 0, \pm 1$ and $k, m = 1, 2, 3$ are the spherical and Cartesian 3-vector components, respectively, and $U^{\rm SC}$ is the transformation matrix from the spherical to the Cartesian coordinates [64]. Equation (47) is the general result for the chiral-odd GPD in baryon states in the $S = T = 1/2$ or $3/2$ representation in leading order of the $1/N_c$ expansion. It covers diagonal and nondiagonal flavor operators ($f' = f$ and $f' \neq f$) and $N \to N, N \to \Delta$, and $\Delta \to \Delta$ transitions.

The general large-N_c matrix element Eq. (47) is now evaluated for the spin-flavor quantum number of the proton, $S = T = S' = T = 1/2$ and $T_3 = T_3' = 1/2$. In this case only the flavor-diagonal matrices $\mathbf{1}$ and τ^3 contribute to the baryon matrix element, and the rotational matrix element Eq. (49b) is given by

$$\langle O^{3i}\rangle_{B'B} = -\frac{1}{3}(\tau^3)_{T_3'T_3}(\sigma^i)_{S_3'S_3} = -\frac{1}{3}(\sigma^i)_{S_3'S_3}. \tag{50}$$

We obtain the proton matrix element in the notation of Eq. (1) as

$$\mathcal{M}^{u+d}_{\rm GPDs}[i\sigma^{+j}] = \frac{2M_N}{\sqrt{2}}\left[\mathbf{1}X_1^j\frac{|\boldsymbol{\Delta}_\perp|}{2M_N}G_{\rm mf,1}\right], \tag{51a}$$

$$\mathcal{M}^{u-d}_{\rm GPDs}[i\sigma^{+j}] = \frac{2M_N}{\sqrt{2}}\left[i\epsilon^{3jm}\sigma^m X_0 G_{\rm mf,0} + i\epsilon^{3jm}\sigma^3 X_1^m\frac{|\boldsymbol{\Delta}_\perp|}{2M_N}\tilde{G}_{\rm mf,1} + i\epsilon^{3jl}\sigma^m X_2^{lm}\frac{|\boldsymbol{\Delta}_\perp|^2}{4M_N^2}G_{\rm mf,2}\right], \tag{51b}$$

where it is understood that $\mathbf{1}$ and σ^i are matrices in the spin quantum numbers S_3 and S_3' [see Eqs. (15)–(17) and Sec. III A]. Equation (51) expresses the proton matrix in terms of the mean-field GPDs. Note that $G_{\rm mf,0}, \tilde{G}_{\rm mf,1}$ and $G_{\rm mf,2}$ multiply the isovector structures emerging from the mean field, and $G_{\rm mf,1}$ the isoscalar structure. In order to connect the mean-field GPDs with the conventional proton GPDs, we compare Eq. (51) with the multipole expansion of the proton matrix element, Eq. (2). In the large-N_c limit the latter becomes

$$\mathcal{M}^{u\pm d}_{\rm GPDs}[i\sigma^{+j}] = \frac{2M_N}{\sqrt{2}}\left\{i\epsilon^{3jm}\sigma^m X_0\left[H_T^{u\pm d} - \left(\frac{|\boldsymbol{\Delta}_\perp|^2}{8M_N^2} + \xi^2\right)E_T^{u\pm d} + \xi\tilde{E}_T^{u\pm d}\right] + \mathbf{1}X_1^j\frac{|\boldsymbol{\Delta}_\perp|}{2M_N}(H_T^{u\pm d} + 2\tilde{H}_T^{u\pm d} + E_T^{u\pm d}) + i\epsilon^{3jm}\sigma^3 X_1^m\frac{|\boldsymbol{\Delta}_\perp|}{2M_N}\left(-\frac{\xi}{2}H_T^{u\pm d} + \tilde{E}_T^{u\pm d} - \xi E_T^{u\pm d}\right) + i\epsilon^{3jl}\sigma^m X_2^{lm}\frac{|\boldsymbol{\Delta}_\perp|^2}{4M_N^2}\left(\frac{1}{2}H_T^{u\pm d} + E_T^{u\pm d}\right)\right\}, \tag{52}$$

where we have simplified the expressions using the N_c scaling of the kinematic variables, Eq. (42). [Equation (52) is the multipole expansion with canonical nucleon spin states, which differs from the one with light-front helicity spin states, Eq. (19), by terms of the order $|\boldsymbol{\Delta}_\perp|/M_N$; the difference is irrelevant in leading order of $1/N_c$ but becomes relevant when considering subleading corrections.] Equation (52) applies to both the flavor-non-singlet and singlet matrix elements. Comparing Eq. (52) with Eq. (51) we obtain relations between the proton GPDs and the mean-field GPDs in the large-N_c limit. In the flavor-non-singlet sector,

$$H_T^{u-d} + \left(\frac{t}{8M_N^2} - \frac{\xi^2}{2}\right)E_T^{u-d} + \xi\tilde{E}_T^{u-d} = G_{\rm mf,0}, \tag{53a}$$

$$H_T^{u-d} + 2\tilde{H}_T^{u-d} + E_T^{u-d} = Z_1, \tag{53b}$$

$$-\frac{\xi}{2}H_T^{u-d} - \xi E_T^{u-d} + \tilde{E}_T^{u-d} = \tilde{G}_{\rm mf,1}, \tag{53c}$$

$$\frac{1}{2}H_T^{u-d} + E_T^{u-d} = G_{\rm mf,2}. \tag{53d}$$

In the flavor-singlet sector

$$H_T^{u+d} + \left(\frac{t}{8M_N^2} - \frac{\xi^2}{2}\right)E_T^{u+d} + \xi\tilde{E}_T^{u+d} = Z_0, \tag{54a}$$

$$H_T^{u+d} + 2\tilde{H}_T^{u+d} + E_T^{u+d} = G_{\rm mf,1}, \tag{54b}$$

$$-\frac{\xi}{2}H_T^{u+d} - \xi E_T^{u+d} + \tilde{E}_T^{u+d} = \tilde{Z}_1, \tag{54c}$$

$$\frac{1}{2}H_T^{u+d} + E_T^{u+d} = Z_2. \tag{54d}$$

Here we have used that in the large-N_c limit [see Eq. (42)]

$$\frac{|\boldsymbol{\Delta}_\perp|^2}{8M_N^2} + \xi^2 = -\frac{t}{8M_N^2} + \frac{\xi^2}{2} + \mathcal{O}(N_c^{-3}). \tag{55}$$

The functions Z_1 in Eq. (53) and $Z_0, \tilde{Z}_1$ and Z_2 in Eq. (54) represent isovector and isoscalar multipoles that are zero in leading order of the $1/N_c$ expansion (i.e., in the static mean field) and become nonzero only at next-to-leading order

(due to rotations of the mean field). The order in $1/N_c$ of these "zero functions" will be established in the following and will result in a set of equations that can be solved consistently within the $1/N_c$ expansion.

C. Scaling behavior and relations

Using the relations Eqs. (53) and (54) we can now establish the N_c scaling of the proton GPDs and derive relations between them. The primary input to this is the N_c scaling of the mean-field GPDs.

In the parametrization of the mean-field matrix element Eq. (44), the mass dimension of the powers of $|\boldsymbol{\Delta}_\perp|$ is compensated by inverse powers of M_N, following standard practice as e.g. in Eq. (2). In the large-N_c limit $M_N = \mathcal{O}(N_c)$, and the powers of M_N influence the N_c scaling of the mean-field GPDs multiplying the structures. It can easily be seen that the functions exhibiting "natural" N_c scaling are

$$G_{\mathrm{mf},0}, \quad \frac{G_{\mathrm{mf},1}}{M_N}, \quad \frac{\tilde{G}_{\mathrm{mf},1}}{M_N}, \quad \frac{G_{\mathrm{mf},2}}{M_N^2}, \tag{56}$$

which have dimension $(\mathrm{mass})^{-n}$ for the multipoles of order $n = 1$ and 2. The physical scale governing these functions is the baryon radius, which is $\mathcal{O}(N_c^0)$ and stable in the large-N_c limit. This circumstance should be kept in mind in the following. To facilitate comparison with the conventional GPDs we present the N_c scaling in terms of the dimensionless functions $G_{\mathrm{mf},0}, G_{\mathrm{mf},1}, \tilde{G}_{\mathrm{mf},1}$ and $G_{\mathrm{mf},2}$, even though their scaling behavior is influenced by the powers of M_N.

The N_c scaling of the mean-field GPDs is posited as

$$\left\{G_{\mathrm{mf},0}, \frac{G_{\mathrm{mf},1}}{M_N}, \frac{\tilde{G}_{\mathrm{mf},1}}{M_N}, \frac{G_{\mathrm{mf},2}}{M_N^2}\right\}(x,\xi,t) \sim N_c^2 \times \mathrm{function}(N_c x, N_c \xi, t). \tag{57}$$

The scaling function does not depend on N_c and is stable in the large-N_c limit; the form of the arguments follows from the scaling of the x and ξ variables, Eqs. (42) and (43) [63]. [It is understood that each GPD has its own scaling function; Eq. (57) and the following formulas indicate the scaling behavior in a compact notation.] The power of N_c multiplying the function is based on several arguments and observations: (i) The power of N_c of the GPDs can be inferred from the N_c scaling of the tensor FFs representing the first moments of the GPDs (see Secs. II and V). (ii) The analysis of GPDs in the general mean-field picture of large-N_c baryons in Sec. V shows that the functions Eq. (57) arise as the sum of quark single-particle matrix elements and have the indicated N_c scaling. (iii) Calculation of the GPDs in the chiral quark-soliton model confirms the N_c scaling, Eq. (57).

Based on Eq. (57), the N_c scaling of the dimensionless mean-field GPDs is obtained as

$$\{G_{\mathrm{mf},0}, G_{\mathrm{mf},1}, \tilde{G}_{\mathrm{mf},1}, G_{\mathrm{mf},2}\}(x,\xi,t) \sim \{N_c^2, N_c^3, N_c^3, N_c^4\} \times \mathrm{function}(N_c x, N_c \xi, t). \tag{58}$$

The functions Z_1 in Eq. (53) and $Z_0, \tilde{Z}_1$ and Z_2 in Eq. (54) parametrize terms in the matrix elements with flavor structure opposite to that of the leading structures parametrized by the mean-field GPDs G_1 and $G_0, \tilde{G}_1$ and G_2, respectively. The scaling behavior in $1/N_c$ of these functions is therefore suppressed by at least one power of $1/N_c$ relative to that of the mean-field GPDs in Eq. (58),

$$\{Z_0, Z_1, \tilde{Z}_1, Z_2\}(x,\xi,t) \sim \{N_c^1, N_c^2, N_c^2, N_c^3\} \times \mathrm{function}(N_c x, N_c \xi, t). \tag{59}$$

Using the scaling assignments of Eqs. (58) and (59) and the systems of Eqs. (53) and (54), we can now derive the N_c scaling of the proton GPDs. In order to isolate the individual proton GPDs a careful analysis is needed, combining the equations in a manner consistent with the parametric order of the terms. In the flavor-non-singlet sector, combining Eqs. (53c) and (53d) we first obtain that $\tilde{E}_T \sim N_c^3$. Using this result, and assuming that E_T is at most $\sim N_c^4$ as allowed by Eq. (53d) (excluding unnatural cancellations), we then determine from Eq. (53a) that $H_T \sim N_c^2$. Carrying this into Eq. (53d), we in turn obtain $E_T \sim N_c^4$. Using this in Eq. (53b), we finally obtain $2\tilde{H}_T + E_T \sim N_c^2$. Because $\tilde{H}_T$ and E_T are individually $\sim N_c^4$, the latter implies the nontrivial relation $2\tilde{H}_T = -E_T + \mathcal{O}(N_c^2)$. Altogether, we obtain the scaling behavior of the leading chiral-odd proton GPDs in the large-N_c limit as

$$\{H_T^{u-d}, \tilde{H}_T^{u-d}, E_T^{u-d}, \tilde{E}_T^{u-d}\}(x,\xi,t) \sim \{N_c^2, N_c^4, N_c^4, N_c^3\} \times \mathrm{function}(N_c x, N_c \xi, t), \tag{60}$$

with the nontrivial relation

$$2\tilde{H}_T^{u-d}(x,\xi,t) = -E_T^{u-d}(x,\xi,t), \tag{61}$$

which is valid up to terms $\sim N_c^2$, i.e., up to relative corrections $\sim 1/N_c^2$ to the functions on each side. In the flavor-singlet sector, in a similar way we obtain

$$\{H_T^{u+d}, \tilde{H}_T^{u+d}, E_T^{u+d}, \tilde{E}_T^{u+d}\}(x,\xi,t) \sim \{N_c, N_c^3, N_c^3, N_c^2\} \times \mathrm{function}(N_c x, N_c \xi, t), \tag{62}$$

and there is no relation analogous to Eq. (61). Equations (60)–(62) establish the N_c scaling of the proton's conventional chiral-odd GPDs as defined by the parametrization, Eq. (1).

Having determined the N_c scaling of the GPDs, we can now "reverse the logic" and express the mean-field GPDs in terms of the conventional GPDs. Simplifying the

relations Eqs. (53) and (54) by using the scaling behavior of Eqs. (60)–(62), we obtain

$$G_{\mathrm{mf},0} = H_T^{u-d} + \left(\frac{t}{8M_N^2} - \frac{\xi^2}{2}\right) E_T^{u-d} + \xi \tilde{E}_T^{u-d}, \tag{63a}$$

$$G_{\mathrm{mf},1} = 2\tilde{H}_T^{u+d} + E_T^{u+d}, \tag{63b}$$

$$\tilde{G}_{\mathrm{mf},1} = -\xi E_T^{u-d} + \tilde{E}_T^{u-d}, \tag{63c}$$

$$G_{\mathrm{mf},2} = E_T^{u-d}. \tag{63d}$$

The combinations on the rhs can be regarded as alternative definitions of the chiral-odd GPDs that have homogeneous N_c scaling and coincide with the mean-field GPDs in the large-N_c limit. Supplemented with the corresponding expressions for the opposite flavor combinations, which are suppressed by a power $1/N_c$, Eq. (63) provides an alternative definition of the full set of chiral-odd GPDs. The new basis has a clear physical interpretation and can be employed in the discussion of nucleon structure and the analysis of exclusive scattering processes. Our subsequent analysis of the chiral-odd GPDs will be conducted in terms of these new GPDs.

The expression of the mean-field GPDs in terms of the conventional GPDs, Eq. (63), combined with the parity in ξ of the conventional GPDs, Eq. (3), implies that the mean-field GPDs have definite parity in ξ. This property will be explored further in Sec. V and Appendix A.

D. Comparison with lattice QCD results

We now want to confront the results of the $1/N_c$ expansion with numerical estimates of chiral-odd GPDs. The most conclusive test can be performed with the large-N_c relation, Eq. (61). It states that the functions $2\tilde{H}_T^{u-d}$ and $-E_T^{u-d}$ are individually large $\mathcal{O}(N_c^4)$ and equal at this order, while their difference is small $\mathcal{O}(N_c^3)$ (see Footnote[2]). This prediction can be compared with lattice QCD results for the tensor FFs and chiral-odd GPDs [48–52].

Figure 2 shows recent lattice QCD results for the flavor-non-singlet GPDs E_T^{u-d} and $-2\tilde{H}_T^{u-d}$ [51]. In this approach the GPDs are extracted by approximating the light cone correlation function of quark fields by an equal-time correlation function in a high-momentum nucleon state; see references in Ref. [51] for details. One sees that the functions E_T^{u-d} and $-2\tilde{H}_T^{u-d}$ are individually large and very close to each other, as stated by the large-N_c relation, Eq. (61). It shows that the $1/N_c$ expansion can provide useful quantitative predictions for the GPDs at $N_c = 3$. We note that the lattice calculation cited here does not control all systematic uncertainties, and that the results likely contain significant higher-twist contributions due to the large values of $|t|/P_z^2$ (see Fig. 2). More stringent comparisons will become possible with more precise lattice QCD results, and with $1/N_c$ corrections to the leading-order expansion.

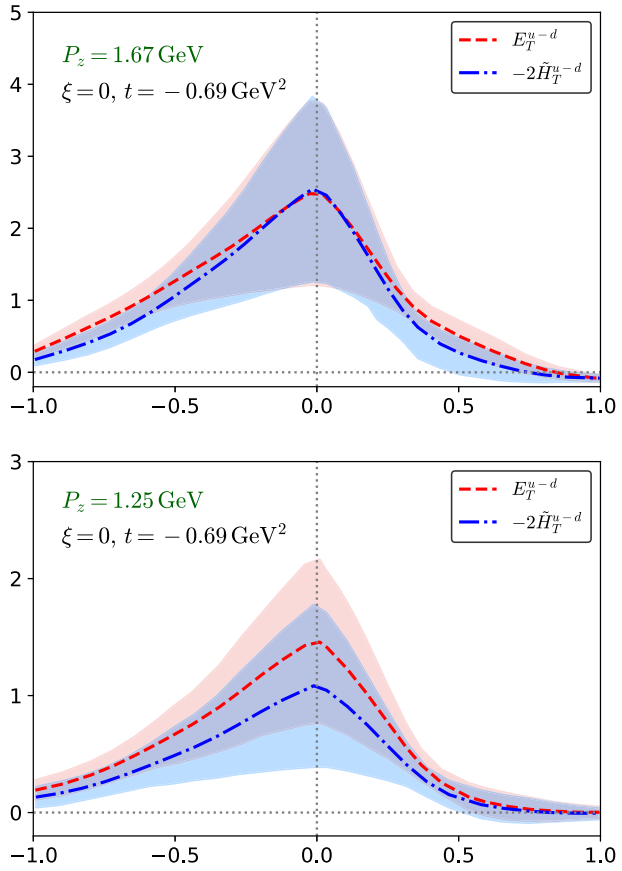

FIG. 2. Comparison between the GPDs E_T^{u-d} (dashed lines) and $-2\tilde{H}_T^{u-d}$ (dot-dashed lines) extracted from the lattice QCD calculation of Ref. [51]. The GPDs are shown as functions of x, at $\xi = 0$ and $t = -0.69\ \mathrm{GeV}^2$, and were extracted from correlation functions with nucleon momenta $P_z = 1.67$ GeV (upper panel) and $P_z = 1.25$ GeV (lower panel). The $1/N_c$ expansion predicts that the two GPDs are the same in leading order; see Eq. (61).

The large-N_c relation Eq. (61) is also supported by the numerical estimates of chiral-odd GPDs in the bag model [65] and a light-front quark model [66]. It is also confirmed by the results of the chiral quark-soliton model, which realizes the large-N_c mean-field picture of baryons with the effective dynamics emerging from chiral symmetry breaking [67].

[2]The parametric order of the corrections to the large-N_c relation Eq. (61) depends on the details of the implementation of the mean-field picture beyond the leading order. In the present calculation with independent translational and rotational zero modes, the corrections appear only at relative order $1/N_c^2$, i.e., suppressed by two powers of $1/N_c$ relative to the leading order. Interplay of the translational and rotational zero modes at subleading order may give rise to relative corrections $1/N_c$. The bag model calculation of Ref. [65] finds corrections of order $1/N_c$. We therefore only claim Eq. (61) to be valid up to relative corrections of order $1/N_c$.

Numerical tests of the large-N_c hierarchy of different spin-flavor structures of the GPDs are less conclusive, because the $1/N_c$ expansion predicts only the parametric order in $1/N_c$, and the numerical values depend on coefficients of order unity. This has been observed in the large-N_c analysis of matrix elements of local operators such as the vector and axial vector currents.

V. POLYNOMIALITY AT LARGE N_c

A. GPDs in mean-field picture

The chiral-odd GPDs satisfy the polynomiality relations, Eq. (5). Their moments are polynomials of degree $\leq m-1$ in ξ and have definite parity in ξ. These properties follow from the fact that the moments are matrix elements of local tensor operators, which are constrained by relativistic covariance and reflection symmetries. In the $1/N_c$ expansion these symmetries are not manifest, as the mean-field breaks translational invariance and exhibits only a generalized form of rotational invariance. It is therefore necessary to study how polynomiality is realized in the $1/N_c$ expansion.

Polynomiality in the mean-field picture is studied most easily by representing the GPDs as matrix elements in quark single-particle states in the mean field. The single-particle motion in the mean-field exhibits a generalized time reversal invariance, which controls the behavior of the GPDs under reflection of ξ. Polynomiality arises from combining this reflection symmetry with the spin-flavor rotational symmetry of mean field. This can be demonstrated in abstract form, with general assumptions about the single-particle motion in the mean field that do not depend on the specific dynamics.

Polynomiality of the GPDs at large N_c was studied in Ref. [47] in the specific dynamics of the chiral quark-soliton model, where the quarks possess a dynamical mass as a result of chiral symmetry breaking, the mean field is a chiral meson field ("soliton"), and the spin-flavor symmetry is realized by the "hedgehog" form of the chiral meson field. In the present study we remain at an abstract level and use only general features that are independent of the specific dynamics [35]. Our aim is to isolate and identify the elements that are needed for ensuring polynomiality of the GPDs. This is useful for generalizing to other realizations of the large-N_c mean-field picture.

We make the following minimal assumptions:

(1) The relativistic motion of the quarks in the mean field of the large-N_c baryon is described by a single-particle Hamiltonian $\hat{H}$ in orbital, spin, and flavor degrees of freedom [35]. The single-particle wave functions and energies are determined by the eigenvalue equation (in bispinor representation)

$$\hat{H}\Phi_n(\boldsymbol{x}) = E_n\Phi_n(\boldsymbol{x}). \tag{64}$$

Here the mean field is centered at the origin and invariant under spatial reflection (parity).

(2) Combined flavor and spatial rotations are generated by the so-called grand spin operator

$$\hat{\boldsymbol{K}} = \hat{\boldsymbol{L}} + \hat{\boldsymbol{\Sigma}} + \hat{\boldsymbol{T}}, \tag{65}$$

where $\hat{\boldsymbol{L}} = \hat{\boldsymbol{x}} \times \hat{\boldsymbol{p}}$ is the orbital angular momentum operator, $\hat{\boldsymbol{\Sigma}}$ the spin operator, and $\hat{\boldsymbol{T}} = \boldsymbol{\tau}/2$ the isospin operator. The invariance of the mean field under such combined rotations implies that the Hamiltonian commutes with the grand spin operator,

$$[\hat{\boldsymbol{K}}, \hat{H}] = 0. \tag{66}$$

The single-particle states are therefore classified by their grand spin eigenvalues K and K_3, in addition to the other quantum numbers characterizing the states (angular momentum, radial quantum number)

$$|n\rangle \equiv |K, K_3, \ldots\rangle. \tag{67}$$

(3) In the ground state of the nucleon, a set of quark single-particle levels is occupied with N_c quarks each, producing a state with total baryon number $B = 1$. Quantities such as the nucleon mass and other observables arise as sum over quark single-particle levels. The precise nature of the single-particle spectrum (discrete or continuous, positive and negative energy states) is not needed in the following.

(4) The matrix elements of the leading-twist partonic operators are given by sums over the occupied quark single-particle states, with the single-particle operators acting only on the single-particle degrees of freedom (position/momentum, spin), without interactions with the rest of system. The leading spin-flavor components of the matrix element in $1/N_c$ are given by single sums over the quark levels. For the chiral-odd partonic operator,

$$\left.\begin{matrix}\mathcal{M}^{u+d}_{\mathrm{GPDs}}[i\sigma^{+j}] \\ \mathcal{M}^{u-d}_{\mathrm{GPDs}}[i\sigma^{+j}]\end{matrix}\right\}$$
$$= 2M_N^2 N_c \left\{ \begin{matrix} \mathbf{1} \\ -\frac{1}{3}\sigma^k \end{matrix} \right\} \sum_{n,\mathrm{occ}} \int \frac{d\lambda}{2\pi} e^{i\lambda(xM_N - E_n)} \int d^3y e^{i\boldsymbol{\Delta}\cdot\boldsymbol{y}}$$
$$\times \Phi_n^\dagger(\boldsymbol{y} + \boldsymbol{e}_3\lambda/2)\gamma^0 i\sigma^{+j} \left\{ \begin{matrix} 1 \\ \tau^k \end{matrix} \right\} \Phi_n(\boldsymbol{y} - \boldsymbol{e}_3\lambda/2). \tag{68}$$

The form follows from the general expression of the mean-field matrix element, Eq. (38). The lightlike separation z in the operator parametrized as

$$z^0 = \lambda, \qquad \boldsymbol{z} = -\lambda\boldsymbol{e}_3. \tag{69}$$

The dependence on z^0 is governed by the time evolution of the single-particle wave function, which is determined by

the single-particle energy E_n in accordance with Eq. (64). "occ" denotes the sum over occupied single-particle levels. In Eq. (68) it is understood that 1 and σ^k are matrices in the nucleon spin quantum numbers S_3' and S_3, as in Eq. (51). The matrix element is for the proton $T_3' = T_3 = 1/2$; for the neutron the isoscalar component remains the same, while the isovector component changes sign.

From Eq. (68), we obtain the mean-field GPDs in the definition of Eqs. (44) and (45) as

$$G_{\rm mf}(x,\xi,t) = 2M_N N_c \sum_{n,\rm occ} \int \frac{d\lambda}{2\pi} e^{i\lambda(xM_N - E_n)} \int d^3y e^{i\boldsymbol{\Delta}\cdot\boldsymbol{y}} \times \Phi_n^\dagger(\boldsymbol{y} + \boldsymbol{e}_3\lambda/2)\hat{O}\Phi_n(\boldsymbol{y} - \boldsymbol{e}_3\lambda/2), \tag{70a}$$

$$\begin{aligned}\hat{O} = & -\frac{1}{12}(1+\gamma^0\gamma^3)i(\boldsymbol{\gamma}\times\boldsymbol{\tau})^3 \quad (\text{for } G_{\rm mf,0}),\\ & -\frac{1}{|\boldsymbol{\Delta}_\perp|^2}(1+\gamma^0\gamma^3)(\boldsymbol{\gamma}_\perp\cdot\boldsymbol{\Delta}_\perp) \quad \left(\frac{G_{\rm mf,1}}{M_N}\right),\\ & -\frac{1}{3|\boldsymbol{\Delta}_\perp|^2}(1+\gamma^0\gamma^3)i(\boldsymbol{\gamma}\times\boldsymbol{\Delta})^3\tau^3 \quad \left(\frac{\tilde{G}_{\rm mf,1}}{M_N}\right),\\ & -\frac{4}{3|\boldsymbol{\Delta}_\perp|^4}(1+\gamma^0\gamma^3)i\left[(\boldsymbol{\gamma}\times\boldsymbol{\Delta})^3(\boldsymbol{\Delta}_\perp\cdot\boldsymbol{\tau}_\perp) - \frac{1}{2}(\boldsymbol{\gamma}\times\boldsymbol{\tau})^3|\boldsymbol{\Delta}_\perp|^2\right] \quad \left(\frac{G_{\rm mf,2}}{M_N^2}\right).\end{aligned} \tag{70b}$$

The 3-momentum transfer $\boldsymbol{\Delta}$ is related to the GPD variables as

$$-2M_N\xi = \Delta^3, \qquad t = -|\boldsymbol{\Delta}|^2, \tag{71}$$

and the N_c scaling of the variables is as specified in Eqs. (41)–(43). Here the mean-field GPDs are represented in first-quantized form, as matrix elements of quark single-particle operators acting only on single-particle variables. The single-particle operators express the multipole character of the respective GPDs. Note that the explicit expressions of the mean-field GPDs in Eq. (70) exhibit the N_c scaling summarized in Eq. (57).

Assumptions 1-4 and the first-quantized representation of the mean-field GPDs of Eq. (70) are our basis for the analysis of polynomiality of the chiral-odd GPDs in the large-N_c limit.

B. Moments in mean-field picture

From Eq. (70) we obtain the moments of the mean-field GPDs in the first-quantized representation as

$$\begin{aligned}&\int dx x^{m-1} G_{\rm mf,0}(x,\xi,t)\\ &= \frac{2N_c i^{m-1}}{M_N^{m-1}} \sum_{n,\rm occ} \int d^3y e^{i\boldsymbol{\Delta}\cdot\boldsymbol{y}} \left(\frac{d}{d\lambda}\right)^{m-1}\\ &\quad \times \left[e^{-i\lambda E_n}\Phi_n^\dagger(\boldsymbol{y}+\boldsymbol{e}_3\lambda/2)\hat{O}\Phi_n(\boldsymbol{y}-\boldsymbol{e}_3\lambda/2)\right]\Big|_{\lambda=0},\end{aligned} \tag{72}$$

and similarly for other the multipoles (see Appendix A). The derivative with respect to the light cone distance λ can be expressed as the action of single-particle momentum operators on the wave functions, similar to the covariant derivatives in the QCD expression, Eq. (5) [47,68,69]. Representing the single-particle wave function in abstract form as

$$\Phi_n(\boldsymbol{x}) \equiv \langle \boldsymbol{x}|n\rangle, \tag{73}$$

and introducing the single-particle momentum operator $\hat{\boldsymbol{p}}$ conjugate to the position operator $\hat{\boldsymbol{x}}$,

$$[\hat{p}^i, \hat{x}^j] = -i\delta^{ij}, \tag{74}$$

the shift in the argument of the single-particle wave function can be represented as

$$\Phi_n(\boldsymbol{y} - \boldsymbol{e}_3\lambda/2) = \langle \boldsymbol{y}|e^{-i\hat{p}^3\lambda/2}|n\rangle. \tag{75}$$

Using the completeness relation

$$\int d^3y e^{i\boldsymbol{\Delta}\cdot\boldsymbol{y}} |\boldsymbol{y}\rangle\langle\boldsymbol{y}| = e^{i\boldsymbol{\Delta}\cdot\hat{\boldsymbol{x}}}, \tag{76}$$

Eq. (72) can be converted to

$$\begin{aligned}&\int dx x^{m-1} G_{\rm mf,0}(x,\xi,t)\\ &= -\frac{1}{6}\frac{M_N N_c}{M_N^m} \sum_{n,\rm occ} \sum_{k=0}^{m-1} \binom{m-1}{k} \frac{E_n^{m-1-k}}{2^k} \sum_{j=0}^{k} \binom{k}{j}\\ &\quad \times \langle n|(1+\gamma^0\gamma^3)i(\boldsymbol{\gamma}\times\boldsymbol{\tau})^3(\hat{p}^3)^j e^{i\boldsymbol{\Delta}\cdot\hat{\boldsymbol{x}}}(\hat{p}^3)^{k-j}|n\rangle\end{aligned} \tag{77}$$

(for the other mean-field GPDs, see Appendix A). Here the moments are expressed as single-particle matrix elements of local operators formed from the single-particle momentum and position operators. A particular feature of the

mean-field description is that the position operator appears explicitly in the expression of the matrix element, resulting from the breaking of translational invariance by the mean field. The function $e^{i\boldsymbol{\Delta}\cdot\hat{\boldsymbol{x}}}$ "pins" the momentum operators on either side, giving rise to a unique structure of the matrix element.

We want to demonstrate that the large-N_c expression of the moment Eq. (77) is a polynomial in ξ of required degree and parity. This can be done using the general features of the mean-field picture listed in the previous subsection and the specific techniques described in the following.

Note that in the moment Eq. (72) the integral over x extends over $[-\infty, \infty]$. In the large-N_c limit, when considering partonic structure in the domain $x = \mathcal{O}(N_c^{-1})$, the range of x is not limited to $[-1, 1]$. Rather, the parton distributions are exponentially small for values $|x| \sim 1 \gg 1/N_c$, so that the integration can be extended over the infinite domain [63,70].

C. Symmetries in mean-field picture

The dynamical symmetries of the mean-field picture play an essential role in the realization of polynomiality. Here we summarize the properties and techniques used in the following calculation.

Time reversal (G_5 *symmetry*): Time reversal and Hermiticity not only impose constraints on the polynomial properties of the GPDs in ξ but also imply the vanishing of the first moments of the GPDs $\tilde{E}_T^f$, Eq. (7d). In the context of the mean-field picture one considers a combination of the standard time-reversal symmetry and an isospin rotation, the so-called G_5 transformation [69]. It is represented by the unitary matrix

$$G_5 = \gamma^1\gamma^3\tau^2, \tag{78}$$

and the following identities hold:

$$G_5\gamma^\mu G_5^{-1} = (\gamma^\mu)^T, \qquad G_5\hat{\Sigma}^i G_5^{-1} = -(\hat{\Sigma}^i)^T, \tag{79a}$$

$$G_5\tau^a G_5^{-1} = -(\tau^a)^T, \tag{79b}$$

$$G_5\hat{H}G_5^{-1} = (\hat{H})^T, \qquad G_5\Phi_n(\boldsymbol{x}) = \Phi_n^*(\boldsymbol{x}). \tag{79c}$$

Using these relations, we can examine the behavior of the matrix elements of the various single-particle operators in Eq. (77). For a general matrix element,

$$\begin{aligned}&\langle n|\Gamma(\hat{p}^3)^l F(\hat{\boldsymbol{x}})(\hat{p}^3)^m|n\rangle \\ &\quad = (-1)^{l+m}\langle n|(G_5\Gamma G_5^{-1})^T(\hat{p}^3)^m F(\hat{\boldsymbol{x}})(\hat{p}^3)^l|n\rangle,\end{aligned} \tag{80}$$

where Γ is a spin-flavor matrix and $F(\hat{\boldsymbol{x}})$ is a general function of the position operator.

Parity ($\hat{\Pi}$ *symmetry*): Parity constrains the form of the chiral-odd GPDs by restricting the allowed angular momentum values in the partial-wave expansion of the single-particle operators. The parity transformation $\hat{\Pi}$ is defined as

$$\hat{\Pi} = \hat{\Pi}^{-1} \equiv \gamma^0\hat{\mathcal{P}}, \qquad \hat{\mathcal{P}}F(\hat{\boldsymbol{x}})\hat{\mathcal{P}}^{-1} = F(-\hat{\boldsymbol{x}}). \tag{81}$$

The mean-field centered at the origin is invariant under parity, so that the Hamiltonian commutes with the parity operator,

$$[\hat{\Pi}, \hat{H}] = 0, \tag{82}$$

and the single-particle states are eigenstates of parity

$$\hat{\Pi}|n\rangle = \pm|n\rangle. \tag{83}$$

The general matrix element Eq. (80) transforms as

$$\begin{aligned}&\langle n|\Gamma(\hat{p}^3)^l F(\hat{\boldsymbol{x}})(\hat{p}^3)^m|n\rangle \\ &= (-1)^{l+m}\langle n|(\gamma^0\Gamma\gamma^0)(\hat{p}^3)^l(\hat{\mathcal{P}}F(\hat{\boldsymbol{x}})\hat{\mathcal{P}}^{-1})(\hat{p}^3)^m|n\rangle.\end{aligned} \tag{84}$$

Partial-wave expansion: The dependence of the moment Eq. (77) on the momentum transfer Δ is contained in the operator function $e^{i\boldsymbol{\Delta}\cdot\hat{\boldsymbol{x}}}$ arising from the quantization of the translational motion of the mean field. The dependence on ξ emerges from the identification of ξ with Δ^3 in the large-N_c kinematics, Eq. (71). In order to exhibit this dependence, we perform a partial-wave expansion of the function $e^{i\boldsymbol{\Delta}\cdot\hat{\boldsymbol{x}}}$ with the 3-axis as a quantization axis (see Refs. [69,71] and Appendix F in Ref. [47]),

$$e^{i\boldsymbol{\Delta}\cdot\hat{\boldsymbol{x}}} = \sum_{l=0}^{\infty} i^l(2l+1)j_l(|\hat{\boldsymbol{x}}||\boldsymbol{\Delta}|)P_l\left(\frac{\hat{x}^3}{|\hat{\boldsymbol{x}}|}\right)P_l\left(\frac{\Delta^3}{|\boldsymbol{\Delta}|}\right), \tag{85}$$

where j_l are the spherical Bessel functions and P_l the Legendre polynomials. In terms of the GPD variables ξ and t, Eq. (71), this becomes

$$\begin{aligned}e^{i\boldsymbol{\Delta}\cdot\hat{\boldsymbol{x}}} = \sum_{l=0}^{\infty} &i^l(2l+1)j_l(|\hat{\boldsymbol{x}}|\sqrt{-t}) \\ &\times P_l\left(\frac{\hat{x}^3}{|\hat{\boldsymbol{x}}|}\right)P_l\left(-\frac{2\xi M_N}{\sqrt{-t}}\right).\end{aligned} \tag{86}$$

In particular, when taking the limit $t \to 0$ while keeping $\xi \neq 0$ fixed, this reduces to

$$\lim_{t\to 0,\xi\neq 0} e^{i\boldsymbol{\Delta}\cdot\hat{\boldsymbol{x}}} = \sum_{l=0}^{\infty}\frac{(-2i\xi M_N|\hat{\boldsymbol{x}}|)^l}{l!}P_l\left(\frac{\hat{x}^3}{|\hat{\boldsymbol{x}}|}\right). \tag{87}$$

Grand spin selection rule: The spin-flavor symmetry of the mean field provides that the quark single-particle states are eigenstates of the grand spin operator, Eq. (67). The mean-field GPDs and the moments Eq. (77) are given by

sums of the expectation values of certain single-particle operators $\hat{O}$ in the single-particle states,

$$\sum_{\text{other}} \sum_{K,K_3} \langle K, K_3, \ldots | \hat{O} | K, K_3, \ldots \rangle, \tag{88}$$

where "other" denotes the summation over the other quantum numbers. Here the left and right state have the same grand spin quantum numbers K and K_3, and the summation includes the grand spin projection K_3. This circumstance implies certain selection rules for the matrix elements of the single-particle operator. For a spherical tensor operator in grand spin quantum numbers, $\hat{O}_{K'K'_3}$, where K' and K'_3 are the grand spin quantum numbers characterizing the tensor components, the summation in Eq. (88) can be performed using the Wigner-Eckart theorem,

$$\begin{aligned}
&\sum_{K,K_3} \langle K, K_3, \ldots | \hat{O}_{K'K'_3} | K, K_3, \ldots \rangle \\
&= \sum_{K,K_3} (-1)^{2K'} \frac{\langle K K_3, K' K'_3 | K K_3 \rangle}{\sqrt{2K+1}} \langle K, \ldots \| \hat{O}_{K'} \| K, \ldots \rangle \\
&= \sum_{K} \sqrt{2K+1} \langle K, \ldots \| \hat{O}_{K'} \| K, \ldots \rangle \delta_{K'0} \delta_{K'_3 0},
\end{aligned} \tag{89}$$

where $\langle K, \ldots \| \hat{O}_{K'} \| K, \ldots \rangle$ denotes the reduced matrix element of the operator. Only the spherical tensor component with total grand spin $K' = 0$ and projection $K'_3 = 0$ can contribute to the expectation value, a consequence of the generalized rotational invariance of the mean field. Since the isospin of the quark single-particle operators is limited (t-channel isospin 0 or 1), the grand spin selection rule restricts the angular momentum of tensor operators that can contribute to the sum over single-particle levels in the mean field.

D. Polynomiality in mean-field picture

Using the symmetry relations from the previous subsection, we can now demonstrate the polynomiality of the chiral-odd GPD moments in the mean-field picture. We present the proof for the monopole GPD $G_{\text{mf},0}$, Eq. (77); the extension to the higher multipole GPDs in Eq. (70) is described in Appendix A. First, we apply the G_5 transformation of Eq. (80) to the single-particle matrix element of Eq. (77) and obtain

$$\begin{aligned}
&\langle n | (1 + \gamma^0\gamma^3) i(\boldsymbol{\gamma} \times \boldsymbol{\tau})^3 (\hat{p}^3)^j e^{i\boldsymbol{\Delta}\cdot\hat{\boldsymbol{x}}} (\hat{p}^3)^{k-j} | n \rangle \\
&= \langle n | (\gamma^0\gamma^3)^{k+1} i(\boldsymbol{\gamma} \times \boldsymbol{\tau})^3 (\hat{p}^3)^j e^{i\boldsymbol{\Delta}\cdot\hat{\boldsymbol{x}}} (\hat{p}^3)^{k-j} | n \rangle.
\end{aligned} \tag{90}$$

Here and in the following we use the fact that

$$(\gamma^0\gamma^3)^{k+1} = \begin{cases} \gamma^0\gamma^3 & k \text{ even}, \\ 1 & k \text{ odd} \end{cases} \tag{91}$$

to write the formulas for even and odd k in a compact form. Next, we perform the partial-wave expansion of the operator function $e^{i\boldsymbol{\Delta}\cdot\hat{\boldsymbol{x}}}$ using Eq. (86) and obtain

$$\begin{aligned}
&\sum_{l=0}^{\infty} i^l (2l+1) P_l\left(-\frac{2\xi M_N}{\sqrt{-t}}\right) \\
&\times \langle n | (\gamma^0\gamma^3)^{k+1} i(\boldsymbol{\gamma} \times \boldsymbol{\tau})^3 \\
&\times (\hat{p}^3)^j j_l(|\hat{\boldsymbol{x}}|\sqrt{-t}) P_l\left(\frac{\hat{x}^3}{|\hat{\boldsymbol{x}}|}\right) (\hat{p}^3)^{k-j} | n \rangle.
\end{aligned} \tag{92}$$

Next, applying the parity transformation Eq. (84), we conclude that only even partial waves ($l = 0, 2, 4, \ldots$) are allowed and replace

$$\sum_{l=0}^{\infty} [\ldots] \to \sum_{l=0,2,4\ldots}^{\infty} [\ldots]. \tag{93}$$

Next, we determine the maximum value of l from the grand spin selection rule, Eq. (89). The spin-flavor part of the single-particle operator in Eq. (92) can be rewritten as

$$\begin{aligned}
&(\gamma^0\gamma^3)^{k+1} i(\boldsymbol{\gamma} \times \boldsymbol{\tau})^3 \\
&= \gamma^0(\boldsymbol{\Sigma} \cdot \boldsymbol{\tau} - \Sigma^3 \tau^3) = \gamma^0(\boldsymbol{\Sigma}_\perp \cdot \boldsymbol{\tau}_\perp) \quad (k \text{ even}),
\end{aligned} \tag{94a}$$

$$= -i(\boldsymbol{\Sigma} \times \boldsymbol{\tau})^3 \gamma^0\gamma^5 \quad (k \text{ odd}), \tag{94b}$$

where we have used

$$\boldsymbol{\Sigma} = -\gamma^0\boldsymbol{\gamma}\gamma_5, \qquad \gamma_5 \equiv -i\gamma^0\gamma^1\gamma^2\gamma^3. \tag{95}$$

The expression for even k, Eq. (94a), corresponds to a sum of structures with t-channel grand spin 0 and 2; the expression for odd k, Eq. (94b), is a structure with grand spin 1. The orbital part of the single-particle operator in Eq. (92), consisting of the functions of the momentum and position operators, has to be coupled to the spin-flavor part to acheive total t-channel grand spin 0, in order to satisfy the selection rule, Eq. (89). The products of powers of $\hat{p}^3$ and $\hat{x}^3$ in Eq. (92) amount to a set of tensor operators with maximum rank $k + l$. The condition that these tensors be reducible to total spin 2 (for even k) or spin 1 (for odd k) fixes the maximum possible value of l for a given k as

$$l_{\max}(k) = k + 2 \quad (k \text{ even}), \tag{96a}$$

$$= k + 1 \quad (k \text{ odd}). \tag{96b}$$

In the representation of the m-th moment in Eq. (77), the values of k are summed over the range $0 \le k \le m - 1$. For a given m, the maximal value of l attained in the partial-wave expansion Eq. (92) is given by $l_{\max}(k = m - 1)$, which according to Eq. (96) is

$$l_{\max}(m) = m+1 \quad (m \text{ odd}), \tag{97a}$$

$$= m \quad (m \text{ even}). \tag{97b}$$

Next, knowing the limits of l in the partial-wave expansion directly in terms of m, we interchange the order of summation over k and l in Eqs. (77) and (92),

$$\sum_{k=0}^{m-1} \sum_{l=0,2,4\ldots}^{l_{\max}(m)} = \sum_{l=0,2,4\ldots}^{l_{\max}(m)} \sum_{k=0}^{m-1}. \tag{98}$$

Finally, after these steps, we can present the moment of the mean-field GPD in Eq. (77) in the form

$$\int dx x^{m-1} G_{\mathrm{mf},0}(x,\xi,t) = \sum_{l=0,2,4\ldots}^{l_{\max}(m)} (2l+1) P_l\left(-\frac{2\xi M_N}{\sqrt{-t}}\right) C^{ml}_{\mathrm{mf},0}(t), \tag{99}$$

where

$$C^{ml}_{\mathrm{mf},0}(t) = -\frac{1}{6}\frac{M_N N_c}{M_N^m} \sum_{n,\mathrm{occ}} \sum_{k=0}^{m-1} \binom{m-1}{k} \frac{E_n^{m-1-k}}{2^k} \sum_{j=0}^{k} \binom{k}{j} \times \langle n|(\gamma^0\gamma^3)^{k+1} i(\boldsymbol{\gamma}\times\boldsymbol{\tau})^3 \times i^l (\hat{p}^3)^j j_l(|\hat{\boldsymbol{x}}|\sqrt{-t}) P_l\left(\frac{\hat{x}^3}{|\hat{\boldsymbol{x}}|}\right) (\hat{p}^3)^{k-j} |n\rangle. \tag{100}$$

These functions are the mean-field generalized FFs in the partial-wave representation of the GPD moments, where the ξ dependence is contained in the Legendre polynomials of angular momentum l.

One observes that the m-th moment of the chiral-odd mean-field GPD $G_{0,\mathrm{mf}}$ is an even polynomial in ξ with degree $m+1$ (for odd m) or m (for even m). These findings agree with the general polynomiality properties Eq. (5) if the mean-field GPD is identified with the conventional chiral-odd GPDs according to Eq. (63a). In particular, the maximum power of ξ in $G_{0,\mathrm{mf}}$ is consistent with the presence of the $\xi^2 E_T^{u-d}$ term in Eq. (63a), which raises the degree of the polynomial by 2 compared to Eq. (5c).

The polynomiality properties of the dipole and quadrupole mean-field GPDs are demonstrated in a similar manner in Appendix A. Altogether our analysis shows that the polynomiality properties of the chiral-odd GPDs are correctly reproduced in the mean-field picture of the nucleon at large N_c.

VI. SUM RULES AT LARGE N_c

A. Spin-flavor structure of tensor FFs

The chiral-odd GPDs are connected with the nucleon tensor FFs through the sum rules, Eq. (7). They follow from the connection of the chiral-odd partonic operator with the local tensor operator and the constraints imposed by relativistic covariance. It is interesting to study how the sum rules are obtained in the large-N_c limit, with the restricted realization of rotational invariance in the mean-field picture. This will also provide explicit expressions for the mean-field tensor FFs and their representation in quark single-particle operators.

The $1/N_c$ expansion of the matrix element of the tensor operator is performed in the Breit frame Eq. (23) using canonical spin states. In analogy to the study of the partonic operator in Sec. IV B, we start from the matrix element of the local tensor operator between large-N_c baryon states with definite momenta but as yet indefinite spin-isospin, referred to as the mean-field matrix element, given by Eq. (38) with $z=0$. The mean-field matrix elements of the $0i$ and ij components of the local tensor operator are parametrized as

$$\langle \boldsymbol{p}', \mathrm{mf}|\bar{\psi}_{f'}(0) i\sigma^{0i} \psi_f(0)|\boldsymbol{p}, \mathrm{mf}\rangle = 2M_N \mathbf{1}_{f'f} Y_1^i \frac{\sqrt{-t}}{2M_N} F_{\mathrm{mf},1}, \tag{101a}$$

$$\langle \boldsymbol{p}', \mathrm{mf}|\bar{\psi}_{f'}(0) i\sigma^{ij} \psi_f(0)|\boldsymbol{p}, \mathrm{mf}\rangle = 2M_N \left[-3i\epsilon^{ijm}(\tau^m)_{f'f} Y_0 F_{\mathrm{mf},0} + 3i\epsilon^{ijl}(\tau^m)_{f'f} Y_2^{lm} \frac{t}{4M_N^2} F_{\mathrm{mf},2}\right], \tag{101b}$$

where

$$F_{\mathrm{mf},0}, F_{\mathrm{mf},1}, F_{\mathrm{mf},2} = \text{functions}(t) \tag{102}$$

are the mean-field FFs, and the subscript denotes the order of the multipole structure in the 3D momentum transfer $\boldsymbol{\Delta}$. Compared to the mean-field GPDs, Eq. (44), there is one less multipole structure. This is because time-reversal invariance for the mean-field GPDs imposes only even/oddness in ξ, while for the mean-field FFs it eliminates one of the multipole structures.

In the next step we project the mean-field matrix elements on definite baryon spin-isospin states, by performing the integral over flavor rotations as in Eqs. (48) and (49). We obtain

$$\mathcal{M}_{\mathrm{FFs}}[i\sigma^{0i}] = 2M_N Y_1^i \mathbf{1}_{f'f} \langle 1\rangle_{B'B} \frac{\sqrt{-t}}{2M_N} F_{\mathrm{mf},1}, \tag{103a}$$

$$\mathcal{M}_{\mathrm{FFs}}[i\sigma^{ij}] = 2M_N (\tau^k)_{f'f} \langle O^{km}\rangle_{B'B} \times \left[-i\epsilon^{ijm} 3F_{\mathrm{mf},0} + i\epsilon^{ijl} Y_2^{lm} \frac{3t}{4M_N^2} F_{\mathrm{mf},2}\right]. \tag{103b}$$

We evaluate the matrix elements for the spin-flavor quantum number of the proton, $S = T = S' = T = 1/2$ and $T_3 = T_3' = 1/2$. In this case only the flavor-diagonal matrices $\mathbf{1}$ and τ^3 contribute, and the rotational matrix elements are given in Eq. (50). We obtain

$$\mathcal{M}^{u+d}_{\mathrm{FFs}}[i\sigma^{0i}] = 2M_N \mathbf{1} Y_1^i \frac{\sqrt{-t}}{2M_N} F_{\mathrm{mf},1}, \tag{104a}$$

$$\mathcal{M}^{u-d}_{\mathrm{FFs}}[i\sigma^{ij}] = 2M_N \left[i\epsilon^{ijm}\sigma^m Y_0 F_{\mathrm{mf},0} - i\epsilon^{ijl}\sigma^m Y_2^{lm} \frac{t}{4M_N^2} F_{\mathrm{mf},2} \right]. \tag{104b}$$

The $0i$ components produce a flavor-singlet structure, the ij components a flavor-non-singlet structure.

In the next step we connect the mean-field FFs to the conventional proton tensor FFs, by comparing the mean-field matrix elements Eq. (104) with the multipole expansion of the proton matrix element Eq. (27). In the large-N_c limit the latter becomes

$$\mathcal{M}^{u\pm d}_{\mathrm{FFs}}[i\sigma^{0j}] = 2M_N \mathbf{1} Y_1^j \frac{\sqrt{-t}}{2M_N} [H_T^{u\pm d} + 2\tilde{H}_T^{u\pm d} + E_T^{u\pm d}], \tag{105a}$$

$$\mathcal{M}^{u\pm d}_{\mathrm{FFs}}[i\sigma^{ij}] = 2M_N \left\{ i\epsilon^{ijk}\sigma^k Y_0 \left[H_T^{u\pm d} + \frac{t}{6M_N^2} E_T^{u\pm d} \right] - i\epsilon^{ijk}\sigma^m Y_2^{km} \frac{t}{4M_N^2} \left[\frac{1}{2} H_T^{u\pm d} + E_T^{u\pm d} \right] \right\}. \tag{105b}$$

Equating Eqs. (105) and (104), we obtain the relations between the mean-field FFs and the tensor FFs in the flavor nonsinglet sector,

$$H_T^{u-d} + \frac{t}{6M_N^2} E_T^{u-d} = F_{\mathrm{mf},0}, \tag{106a}$$

$$H_T^{u-d} + 2\tilde{H}_T^{u-d} + E_T^{u-d} = N_1, \tag{106b}$$

$$\frac{1}{2} H_T^{u-d} + E_T^{u-d} = F_{\mathrm{mf},2}, \tag{106c}$$

and in the flavor-singlet sector

$$H_T^{u+d} + \frac{t}{6M_N^2} E_T^{u+d} = N_0, \tag{107a}$$

$$H_T^{u+d} + 2\tilde{H}_T^{u+d} + E_T^{u+d} = F_{\mathrm{mf},1}, \tag{107b}$$

$$\frac{1}{2} H_T^{u+d} + E_T^{u+d} = N_2. \tag{107c}$$

In analogy to the corresponding relations for the GPDs, the functions N_1 in Eq. (106) and N_0 and N_2 in Eq. (107) represent isovector and isoscalar multipoles that are zero in leading order of the $1/N_c$ expansion.

From the relations Eqs. (106) and (107) we now determine the N_c scaling of the proton tensor FFs. Based on similar arguments as for the GPDs in Eq. (56), we posit that the natural N_c scaling of the mean-field FFs is

$$\left\{ F_{\mathrm{mf},0}, \frac{F_{\mathrm{mf},1}}{M_N}, \frac{F_{\mathrm{mf},2}}{M_N^2} \right\}(t) \sim N_c^1 \times \mathrm{function}(t), \tag{108}$$

and that the scaling of the dimensionless mean-field FFs is therefore

$$\{F_{\mathrm{mf},0}, F_{\mathrm{mf},1}, F_{\mathrm{mf},2}\}(t) \sim \{N_c^1, N_c^2, N_c^3\} \times \mathrm{function}(t). \tag{109}$$

These FFs parametrize the leading spin-flavor components of the matrix element in the large-N_c limit. The corresponding "other" flavor components of the matrix element are suppressed by one power of $1/N_c$, so that

$$\{N_0, N_1, N_2\}(t) \sim \{N_c^0, N_c^1, N_c^2\} \times \mathrm{function}(t). \tag{110}$$

The scaling behavior of the conventional FFs is established by solving Eqs. (106) and (107) with the scaling of Eqs. (109) and (110) as input. We obtain

$$\{H_T^{u-d}, \tilde{H}_T^{u-d}, E_T^{u-d}\}(t) \sim \{N_c^1, N_c^3, N_c^3\} \times \mathrm{function}(t), \tag{111a}$$

$$\{H_T^{u+d}, \tilde{H}_T^{u+d}, E_T^{u+d}\}(t) \sim \{N_c^0, N_c^2, N_c^2\} \times \mathrm{function}(t), \tag{111b}$$

and the nontrivial large-N_c relation

$$2\tilde{H}_T^{u-d}(t) = -E_T^{u-d}(t). \tag{112}$$

It is natural that the tensor FFs in Eq. (111) scale with one power less in N_c compared to the chiral-odd GPDs in Eqs. (60) and (62). The FFs are the first moments of the GPDs, and the integral over $x = \mathcal{O}(N_c^{-1})$ reduces the power of N_c of the GPDs by 1 [see Eq. (43)]. This statement can be generalized to the m-th moments of the GPDs,

$$\int dx x^{m-1} \{H_T^{u-d}, \tilde{H}_T^{u-d}, E_T^{u-d}, \tilde{E}_T^{u-d}\} = \{N_c^{2-m}, N_c^{4-m}, N_c^{4-m}, N_c^{3-m}\} \times \mathrm{function}(t), \tag{113a}$$

$$\int dx x^{m-1} \{H_T^{u+d}, \tilde{H}_T^{u+d}, E_T^{u+d}, \tilde{E}_T^{u+d}\} = \{N_c^{1-m}, N_c^{3-m}, N_c^{3-m}, N_c^{2-m}\} \times \mathrm{function}(t). \tag{113b}$$

Finally, applying the N_c scaling Eq. (111) of the tensor FFs to Eqs. (106) and (107), we obtain the connection between the tensor FFs and the mean-field FFs as

$$F_{\mathrm{mf},0} = H_T^{u-d} + \frac{t}{6M_N^2} E_T^{u-d}, \tag{114a}$$

$$F_{\mathrm{mf},1} = E_T^{u+d} + 2\tilde{H}_T^{u+d}, \tag{114b}$$

$$F_{\mathrm{mf},2} = E_T^{u-d}. \tag{114c}$$

B. Tensor FFs in mean-field picture

To verify the sum rules of the GPDs in the large-N_c limit, we need to know how the tensor FFs are expressed as matrix elements of quark single-particle operators in the mean field, in the same way as the GPDs in Sec. V. Using the same assumption as for the partonic operator in Sec. V, we posit that the leading isoscalar and isovector components of the matrix element of the local tensor operator are given by

$$\mathcal{M}_{\mathrm{FFs}}^{u+d}[i\sigma^{0k}] = 2M_N N_c \mathbf{1} \sum_{n,\mathrm{occ}} \langle n|\gamma^0 i\sigma^{0k} e^{i\boldsymbol{\Delta}\cdot\hat{\mathbf{x}}}|n\rangle, \tag{115a}$$

$$\mathcal{M}_{\mathrm{FFs}}^{u-d}[i\sigma^{ij}] = -\frac{2}{3} M_N N_c \sigma^k \sum_{n,\mathrm{occ}} \langle n|\tau^k\gamma^0 i\sigma^{ij} e^{i\boldsymbol{\Delta}\cdot\hat{\mathbf{x}}}|n\rangle. \tag{115b}$$

These expressions can also be obtained by integrating the matrix element of the partonic operator, Eq. (68), over x. Here again the momentum transfer to the mean field is represented by the operator $e^{i\boldsymbol{\Delta}\cdot\hat{\mathbf{x}}}$ in the single-particle matrix elements. The expressions of the mean-field FFs are extracted by performing a 3D multipole expansion in $\boldsymbol{\Delta}$ and separating the spin components of the matrix element Eq. (115). We obtain

$$F_{\mathrm{mf},0}(t) = -\frac{N_c}{9} \sum_{n,\mathrm{occ}} \langle n|\gamma^0(\boldsymbol{\Sigma}\cdot\boldsymbol{\tau}) j_0(|\hat{\mathbf{x}}||\boldsymbol{\Delta}|)|n\rangle, \tag{116a}$$

$$F_{\mathrm{mf},1}(t) = 2M_N N_c \sum_{n,\mathrm{occ}} \langle n|\gamma^0\gamma^5\Sigma^i Y_1^i(\Omega_{\hat{\mathbf{x}}}) \frac{i j_1(|\hat{\mathbf{x}}||\boldsymbol{\Delta}|)}{|\boldsymbol{\Delta}|}|n\rangle, \tag{116b}$$

$$F_{\mathrm{mf},2}(t) = 2M_N^2 N_c \sum_{n,\mathrm{occ}} \langle n|\gamma^0\Sigma^i\tau^j Y_2^{ij}(\Omega_{\hat{\mathbf{x}}}) \frac{j_2(|\hat{\mathbf{x}}||\boldsymbol{\Delta}|)}{|\boldsymbol{\Delta}|^2}|n\rangle, \tag{116c}$$

where $t = -|\boldsymbol{\Delta}|^2$; see Eq. (71). In the forward limit the tensor FFs define the tensor charge $F_{\mathrm{mf},0}(0) = g_T^{u-d}$, the anomalous tensor magnetic moment $F_{\mathrm{mf},1}(0) = \kappa_T^{u+d}$, and the tensor quadrupole moment $F_{\mathrm{mf},2}(0) = E_T(0)$. Their first-quantized expressions are obtained by taking the limit $|\boldsymbol{\Delta}| \to 0$ in Eq. (116),

$$F_{\mathrm{mf},0}(0) = -\frac{N_c}{9} \sum_{n,\mathrm{occ}} \langle n|\gamma^0(\boldsymbol{\Sigma}\cdot\boldsymbol{\tau})|n\rangle, \tag{117a}$$

$$F_{\mathrm{mf},1}(0) = \frac{2M_N N_c}{3} \sum_{n,\mathrm{occ}} \langle n|\gamma^0\gamma^5 i\boldsymbol{\Sigma}\cdot\hat{\mathbf{x}}|n\rangle, \tag{117b}$$

$$F_{\mathrm{mf},2}(0) = \frac{2M_N^2 N_c}{15} \sum_{n,\mathrm{occ}} \langle n|\gamma^0 \left[(\boldsymbol{\Sigma}\cdot\hat{\mathbf{x}})(\boldsymbol{\tau}\cdot\hat{\mathbf{x}}) - \frac{1}{3}(\boldsymbol{\Sigma}\cdot\boldsymbol{\tau})\hat{\mathbf{x}}^2\right]|n\rangle. \tag{117c}$$

The numerical values of these quantities have been estimated in the chiral quark-soliton model in Refs. [72–74].

C. Sum rules for chiral-odd GPDs

We are now in a position to prove the sum rules for the chiral-odd GPDs in the large-N_c limit. To do so, we take the first moment of the mean-field GPDs in the first-quantized representation and connect them with the tensor FFs in Eq. (116), making use of the symmetries of the mean field.

Monopole GPD: The first moment of the monopole GPD is given by Eq. (99) with $m = 1$,

$$\begin{aligned}
&\int dx G_{\mathrm{mf},0}(x,\xi,t) \\
&= -\frac{N_c}{6} \sum_{n,\mathrm{occ}} \Bigg[\langle n|(\gamma^0\gamma^3) i(\boldsymbol{\gamma}\times\boldsymbol{\tau})^3 j_0(|\hat{\mathbf{x}}|\sqrt{-t})|n\rangle \\
&\quad - \frac{15}{2} P_2\left(-\frac{2\xi M_N}{\sqrt{-t}}\right) \langle n|(\gamma^0\gamma^3) i(\boldsymbol{\gamma}\times\boldsymbol{\tau})^3 \\
&\quad \times Y_2^{33}(\Omega_{\hat{\mathbf{x}}}) j_2(|\hat{\mathbf{x}}|\sqrt{-t})|n\rangle \Bigg],
\end{aligned} \tag{118}$$

where the spin-flavor operator can also be expressed as [see Eq. (94a)]

$$(\gamma^0\gamma^3) i(\boldsymbol{\gamma}\times\boldsymbol{\tau})^3 = \gamma^0(\boldsymbol{\Sigma}\cdot\boldsymbol{\tau} - \Sigma^3\tau^3). \tag{119}$$

The first quantized operator in Eq. (118) has a specific orientation with respect to the 3-axis. Since the mean field has spherical symmetry in combined position and isospin space, the averages of the oriented components can be converted to a manifestly spherically symmetric way. Specifically,

$$\tau^3\Sigma^3 = \frac{1}{3}\boldsymbol{\tau}\cdot\boldsymbol{\Sigma} + \ldots, \tag{120a}$$

$$Y_2^{33}\tau^3\Sigma^3 = \frac{2}{15} Y_2^{ij}\tau^i\Sigma^j + \ldots, \tag{120b}$$

where the ellipsis denotes structures with t-channel grand spin > 0, which average to zero because of the selection

rule, Eq. (89). We obtain

$$\int dx G_{\mathrm{mf},0}(x,\xi,t) = -\frac{N_c}{9}\sum_{n,\mathrm{occ}}\langle n|\gamma_0(\boldsymbol{\Sigma}\cdot\boldsymbol{\tau})j_0(|\hat{\boldsymbol{x}}|\sqrt{-t})|n\rangle + \left(\frac{1}{12}+\frac{\xi^2 M_N^2}{t}\right)N_c\sum_{n,\mathrm{occ}} \times \langle n|\gamma^0\Sigma^i\tau^j Y_2^{ij}(\Omega_{\hat{\boldsymbol{x}}})j_2(|\hat{\boldsymbol{x}}|\sqrt{-t})|n\rangle. \tag{121}$$

This spherically symmetric expression of the mean-field GPD moment can be compared with the first-quantized expressions of the mean-field tensor FFs, Eq. (116),

$$\int dx G_{\mathrm{mf},0}(x,\xi,t) = F_{\mathrm{mf},0}(t) - \left(\frac{t}{24M_N^2}+\frac{\xi^2}{2}\right)F_{\mathrm{mf},2}(t) = H_T^{u-d}(t) + \left(\frac{t}{8M_N^2}-\frac{\xi^2}{2}\right)E_T^{u-d}(t). \tag{122}$$

In the last line we have substituted the expression of the mean-field FFs in terms of the conventional FFs of Eq. (114). One observes that this result agrees with the general expression of the first moment of $G_{\mathrm{mf},0}$ that one obtains by expressing the mean-field GPD in terms of the conventional GPDs. It shows the overall consistency of the approach: the first-quantized mean-field expressions reproduce the general sum rules obeyed by the $1/N_c$ expanded GPDs and FFs. Interestingly, the mean-field result Eq. (122) indeed delivers a ξ^2 term in the first moment of the monopole GPD $G_{\mathrm{mf},0}$, as required by the presence of the $\xi^2 E_T^{u-d}$ term in Eq. (63a). It also correctly reproduces the vanishing first moment of $\xi\tilde{E}_T^{u-d}$.

The sum rules for the dipole and quadrupole mean-field GPDs are proved in a similar manner in Appendix B. Altogether our analysis shows that the sum rules for the chiral-odd GPDs are correctly realized in the mean-field picture of the nucleon at large N_c.

VII. CONCLUSIONS AND EXTENSIONS

We have performed a comprehensive study of the nonperturbative properties of the nucleon's chiral-odd GPDs in the large N_c limit of QCD. This includes the parametric ordering of the spin-flavor components, the polynomiality property of the moments, and the sum rules connecting the GPDs with the tensor FFs. The main findings can be summarized as follows.

(i) *Multipole structure*: The chiral-odd GPDs contain monopole, dipole, and quadrupole structures in the transverse momentum transfer $\boldsymbol{\Delta}_\perp$. The presence of the quadrupole structure follows from longitudinal angular momentum conservation in the light-front representation and is confirmed by comparison with the multipole expansion of the matrix elements of the local tensor operators. The quadrupole structure is unique to the chiral-odd GPDs and absent in the chiral-even GPDs.

(ii) $1/N_c$ *expansion*: The nucleon matrix element of the chiral-odd partonic operator in the large-N_c limit is characterized by four independent mean-field GPDs. This corrects the earlier analysis of Ref. [42], which assumed three independent GPDs because it did not include the quadrupole structure. As a result, all four chiral-odd nucleon GPDs can be derived from large-N_c mean-field GPDs without degeneracies, and their N_c scaling is determined completely.

(iii) *Large-N_c relation*: The leading flavor-non-singlet GPDs E_T^{u-d} and $\tilde{H}_T^{u-d}$ are connected by the nontrivial large-N_c relation Eq. (61). The relation is well satisfied by numerical results from recent lattice QCD calculations (see Fig. 2).

(iv) *Polynomiality*: The polynomiality of the moments of the chiral-odd GPDs is fulfilled with the restricted realization of translational and rotational invariance in the mean-field picture of the nucleon at large N_c. Our analysis exhibits precisely what elements of the abstract mean-field picture are responsible for ensuring polynomiality (discrete symmetries, triangle rule for angular momentum addition).

(v) *Sum rules*: The sum rules connecting the chiral-odd GPDs with the FFs of the local tensor operator are satisfied in the large-N_c limit. The presence of the quadrupole structure in the mean-field matrix elements is essential for ensuring the correspondence between the matrix elements of the nonlocal partonic and local tensor operators.

Altogether, our theoretical study shows that the essential qualitative features of the chiral-odd GPDs are correctly reproduced in the general mean-field picture of the nucleon in the large-N_c limit of QCD. This provides a basis for quantitative estimates of the chiral-odd GPDs with specific dynamical realizations of the mean-field picture, such as the chiral quark-soliton model. It also enables a model-independent phenomenological analysis of chiral-odd GPDs and exclusive processes incorporating large-N_c constraints, such as the hierarchy of spin-flavor components of the GPDs.

The studies presented here could be extended in several directions. The spin-flavor symmetry of baryons in the large-N_c limit of QCD naturally connects the $N \to N$ with the $N \to \Delta$ (and even $\Delta \to \Delta$) transition matrix elements of the same QCD operator [75]. This connection could be used to predict the chiral-odd $N \to \Delta$ transition GPDs in terms of the chiral-odd $N \to N$ GPDs, in analogy to what was done with the chiral-even GPDs [1]. The chiral-odd $N \to \Delta$ GPDs are sampled in exclusive pion production processes with $N \to \Delta$ transitions [76], assuming the

chiral-odd twist-3 mechanism that was proposed and tested for $N \to N$ exclusive pion production [15–18]; first measurements have been performed at JLab [75,77]. Measurements of the $N \to \Delta$ transition GPDs can serve as additional tests of the spin-flavor structure predicted by the $1/N_c$ expansion and access structures that are difficult to separate in $N \to N$ measurements alone. In the chiral-odd sector such studies are particularly promising because the operators are pure nonsinglets, and there is no singlet contribution in the $N \to N$ channel that would affect the comparison between $N \to N$ and $N \to \Delta$.

The multipole expansion of the partonic matrix elements developed here could be applied also to higher-twist structures, e.g. the chiral-odd twist-3 structures connected with spin-orbit correlations [78].

The predictive power of the $1/N_c$ expansion could be greatly increased by computing subleading corrections to the nucleon matrix elements. Subleading spin-flavor structures appear due to the finite angular velocity of the collective rotations of the mean field; in the abstract formulation of Sec. IV they could be captured by including terms proportional to the angular velocity in the parametrization of the mean-field matrix elements. In addition, there are $1/N_c$ corrections to the spin-flavor structures that are nonzero in leading order; see Ref. [41] for a review. Both types of corrections involve new dynamical input beyond the mean-field expectation values. This input can be provided by dynamical models such as the chiral quark-soliton model. If lattice QCD calculations were available at different values of N_c, the dynamical input for subleading $1/N_c$ corrections could be assembled model independently, substantially expanding the reach of the $1/N_c$ expansion.

The investigations of the polynomiality of the GPDs presented here focus on how the property arises from the mean-field picture of baryons in the large-N_c limit. The polynomiality of the GPDs can also be realized explicitly using the double distribution representation, a spectral representation of the matrix element of the partonic operator in which the light cone momenta P^+ and Δ^+ (see Sec. II) are regarded as independent variables [1–4]; see Ref. [79] for a topical discussion. Whether this representation could be connected with the mean-field picture and employed for the $1/N_c$ expansion of the GPDs presents an interesting question for further study.

ACKNOWLEDGMENTS

We thank Peter Schweitzer and Kemal Tezgin for a critical reading of an earlier version of the article and helpful comments and suggestions. This material is based upon work supported by the U.S. Department of Energy, Office of Science, Office of Nuclear Physics under Contract No. DE-AC05-06OR23177. The research reported here takes place in the context of the Topical Collaboration "3D quark-gluon structure of hadrons: mass, spin, tomography" (Quark-Gluon Tomography Collaboration) supported by the U.S. Department of Energy, Office of Science, Office of Nuclear Physics under Contract No. DE-SC0023646.

DATA AVAILABILITY

No data were created or analyzed in this study.

APPENDIX A: POLYNOMIALITY OF MULTIPOLE GPDs

1. ξ-even dipole GPD

In this appendix we demonstrate the polynomiality properties of the higher-multipole chiral-odd GPDs in the large-N_c limit. As in the analysis of the monopole GPD in Sec. V D, we take the first-quantized expressions of the mean-field GPDs in Eq. (70), compute the moments as in Eq. (77), and convert the results to a form that explicitly shows the polynomiality in ξ. For simplicity we take $t = 0$ in the analysis of the higher multipole GPDs; the extension to finite t is straightforward.

The m-th moment of the dipole mean-field GPD $G_{\mathrm{mf},1}$ in Eq. (70) is obtained as

$$\begin{aligned}&\int dx x^{m-1} G_{\mathrm{mf},1}(x,\xi,t)\\ &= -\frac{2M_N^2 N_c}{M_N^m |\boldsymbol{\Delta}_\perp|^2} \sum_{n,\mathrm{occ}} \sum_{k=0}^{m-1} \binom{m-1}{k} \frac{E_n^{m-1-k}}{2^k} \sum_{j=0}^{k} \binom{k}{j}\\ &\quad \times \langle n|(1+\gamma^0\gamma^3)(\boldsymbol{\gamma}_\perp \cdot \boldsymbol{\Delta}_\perp)(\hat{p}^3)^j e^{i\boldsymbol{\Delta}\cdot\hat{\boldsymbol{x}}}(\hat{p}^3)^{k-j}|n\rangle. \end{aligned} \tag{A1}$$

Under the G_5 transformation Eq. (80) the single-particle matrix element transforms as

$$\begin{aligned}&\langle n|(1+\gamma^0\gamma^3)(\boldsymbol{\gamma}_\perp \cdot \boldsymbol{\Delta}_\perp)(\hat{p}^3)^j e^{i\boldsymbol{\Delta}\cdot\hat{\boldsymbol{x}}}(\hat{p}^3)^{k-j}|n\rangle\\ &\quad = \langle n|(\gamma^0\gamma^3)^k(\boldsymbol{\gamma}_\perp \cdot \boldsymbol{\Delta}_\perp)(\hat{p}^3)^j e^{i\boldsymbol{\Delta}\cdot\hat{\boldsymbol{x}}}(\hat{p}^3)^{k-j}|n\rangle. \end{aligned} \tag{A2}$$

Here we use a notation analogous to Eq. (91),

$$(\gamma^0\gamma^3)^k = \begin{cases} 1 & k \text{ even}, \\ \gamma^0\gamma^3 & k \text{ odd}; \end{cases} \tag{A3}$$

note that the even/odd pattern is opposite to the one in the monopole GPD Eq. (90). Performing the partial-wave expansion of the function $e^{i\boldsymbol{\Delta}\cdot\hat{\boldsymbol{x}}}$ in Eq. (A2) in the limit $t \to 0$ [see Eq. (87)], and replacing the factor $1/|\boldsymbol{\Delta}_\perp|^2$ by [see Eq. (71)]

$$\frac{1}{|\boldsymbol{\Delta}_\perp|^2} = \frac{1}{-t-(2\xi M_N)^2} \overset{t\to 0}{=} -\frac{1}{(2\xi M_N)^2}, \tag{A4}$$

we obtain

$$\lim_{t\to 0,\,\xi\neq 0}\sum_{l=2}^{\infty}\langle n|(\gamma^0\gamma^3)^k(\hat{p}^3)^j i(\boldsymbol{\nabla}_\perp\cdot\boldsymbol{\gamma}_\perp) \times\left[\frac{(-2i\xi M_N|\hat{\boldsymbol{x}}|)^l}{(2\xi M_N)^2 l!}P_l\left(\frac{\hat{x}^3}{|\hat{\boldsymbol{x}}|}\right)\right](\hat{p}^3)^{k-j}|n\rangle. \quad \text{(A5)}$$

Here the momentum transfer $\boldsymbol{\Delta}_\perp$ in Eq. (A2) has been replaced by a derivative acting on the function $e^{i\boldsymbol{\Delta}\cdot\hat{\boldsymbol{x}}}$,

$$\begin{aligned}\lim_{t\to 0,\,\xi\neq 0}\Delta^i_\perp e^{i\boldsymbol{\Delta}\cdot\hat{\boldsymbol{x}}} &= \lim_{t\to 0,\,\xi\neq 0}[\hat{p}^i_\perp, e^{i\boldsymbol{\Delta}\cdot\hat{\boldsymbol{x}}}]\\ &= \lim_{t\to 0,\,\xi\neq 0} -i\nabla^i_\perp e^{i\boldsymbol{\Delta}\cdot\hat{\boldsymbol{x}}}\\ &= -i\sum_{l=2}^{\infty}\nabla^i_\perp\left[\frac{(-2i\xi M_N|\hat{\boldsymbol{x}}|)^l}{l!}P_l\left(\frac{\hat{x}^3}{|\hat{\boldsymbol{x}}|}\right)\right].\end{aligned} \quad \text{(A6)}$$

Note that the summation over l in Eq. (A5) starts from $l=2$ because

$$\left[\hat{p}^i_\perp, |\hat{\boldsymbol{x}}|P_1\left(\frac{\hat{x}^3}{|\hat{\boldsymbol{x}}|}\right)\right]=0. \quad \text{(A7)}$$

Because of parity invariance Eq. (84), the allowed partial waves in Eq. (A5) are even, $l=2,4,\ldots$, and the sum becomes

$$\sum_{l=2}^{\infty}[\ldots]\to\sum_{l=2,4\ldots}^{\infty}[\ldots]. \quad \text{(A8)}$$

The spin part of the single-particle operator in Eq. (A2) can be rewritten as

$$\begin{aligned}&(\gamma^0\gamma^3)^k\boldsymbol{\gamma}_\perp\cdot\boldsymbol{\nabla}_\perp\\ &=\boldsymbol{\gamma}_\perp\cdot\boldsymbol{\nabla}_\perp=-\gamma^0\gamma^5(\boldsymbol{\Sigma}_\perp\cdot\boldsymbol{\nabla}_\perp)\quad (k\text{ even}),\\ &=\gamma^0\gamma^3\boldsymbol{\gamma}_\perp\cdot\boldsymbol{\nabla}_\perp=\gamma^0 i(\boldsymbol{\Sigma}\times\boldsymbol{\nabla})^3\quad (k\text{ odd}).\end{aligned} \quad \text{(A9)}$$

Using the grand spin selection rule and Eq. (A9), following the same logic as in the derivation of Eq. (96), the maximum value of l in the sum of Eq. (A5) is determined as

$$l_{\max}(k)=k+2\quad (k\text{ even}), \quad \text{(A10a)}$$

$$=k+1\quad (k\text{ odd}). \quad \text{(A10b)}$$

In terms of m, the maximum value is given by $l_{\max}(k=m-1)$. It is convenient to change the summation variable in Eq. (A5) from l to $l-2$, so that it represents the actual powers of ξ in the polynomial. The maximum value of the new variable is then given by

$$l_{\max}(m)=m-1\quad (m\text{ odd}), \quad \text{(A11a)}$$

$$=m-2\quad (m\text{ even}). \quad \text{(A11b)}$$

Altogether we obtain the moment of the dipole mean-field GPD $G_{\mathrm{mf},1}$ as

$$\int dx x^{m-1}G_{\mathrm{mf},1}(x,\xi,0)=\sum_{l=0,2\ldots}^{l_{\max}(m)}\xi^l C^{ml}_{\mathrm{mf},1}(t=0), \quad \text{(A12)}$$

where the generalized mean-field FFs are given by

$$\begin{aligned}C^{ml}_{\mathrm{mf},1}(t=0)=&-\frac{N_c}{2M_N^m}\sum_{n,\mathrm{occ}}\sum_{k=0}^{m-1}\binom{m-1}{k}\frac{E_n^{m-1-k}}{2^k}\sum_{j=0}^{k}\binom{k}{j}\\ &\times\langle n|(\gamma^0\gamma^3)^k(\hat{p}^3)^j i(\boldsymbol{\nabla}_\perp\cdot\boldsymbol{\gamma}_\perp)\\ &\times\left[\frac{(-2iM_N|\hat{\boldsymbol{x}}|)^{l+2}}{(l+2)!}P_{l+2}\left(\frac{\hat{x}^3}{|\hat{\boldsymbol{x}}|}\right)\right](\hat{p}^3)^{k-j}|n\rangle.\end{aligned} \quad \text{(A13)}$$

Equation (A12) shows that the moments of the dipole mean-field GPD $G_{\mathrm{mf},1}$ are even polynomials in ξ, with a degree given by Eq. (A11). This agrees with the polynomiality properties required by the identification of the mean-field GPD with the conventional GPDs, Eqs. (5) and (63).

2. ξ-odd dipole GPD

The m-th moment of the dipole mean-field GPD $\tilde{G}_{\mathrm{mf},1}$ in Eq. (70) is obtained as

$$\begin{aligned}&\int dx x^{m-1}\tilde{G}_{\mathrm{mf},1}(x,\xi,t)\\ &=\frac{2}{3}i\frac{M_N^2N_c}{M_N^m|\boldsymbol{\Delta}_\perp|^2}\sum_{n,\mathrm{occ}}\sum_{k=0}^{m-1}\binom{m-1}{k}\frac{E_n^{m-1-k}}{2^k}\sum_{j=0}^{k}\binom{k}{j}\\ &\times\langle n|(1+\gamma^0\gamma^3)\tau^3(\hat{p}^3)^j(\boldsymbol{\Delta}\times\boldsymbol{\gamma})^3e^{i\boldsymbol{\Delta}\cdot\hat{\boldsymbol{x}}}(\hat{p}^3)^{k-j}|n\rangle.\end{aligned} \quad \text{(A14)}$$

Under the G_5 transformation Eq. (80) the single-particle matrix element transforms as

$$\begin{aligned}&\langle n|(1+\gamma^0\gamma^3)\tau^3(\hat{p}^3)^j(\boldsymbol{\Delta}\times\boldsymbol{\gamma})^3e^{i\boldsymbol{\Delta}\cdot\hat{\boldsymbol{x}}}(\hat{p}^3)^{k-j}|n\rangle\\ &=\langle n|(\gamma^0\gamma^3)^{k+1}\tau^3(\hat{p}^3)^j(\boldsymbol{\Delta}\times\boldsymbol{\gamma})^3e^{i\boldsymbol{\Delta}\cdot\hat{\boldsymbol{x}}}(\hat{p}^3)^{k-j}|n\rangle,\end{aligned} \quad \text{(A15)}$$

where we use the same notation as in Eq. (91). Performing the partial-wave expansion of the function $e^{i\boldsymbol{\Delta}\cdot\hat{\boldsymbol{x}}}$ at $t=0$, treating the factor $1/|\boldsymbol{\Delta}_\perp|^2$ as in Eq. (A4), we obtain

$$\lim_{t\to 0,\,\xi\neq 0}-\sum_{l=2}^{\infty}\langle n|(\gamma^0\gamma^3)^{k+1}\tau^3(\hat{p}^3)^j(\boldsymbol{\nabla}\times\boldsymbol{\gamma})^3 \times\left[\frac{(-2i\xi M_N|\hat{\boldsymbol{x}}|)^l}{(2\xi M_N)^2 l!}P_l\left(\frac{\hat{x}^3}{|\hat{\boldsymbol{x}}|}\right)\right](\hat{p}^3)^{k-j}|n\rangle. \quad \text{(A16)}$$

Here the momentum transfer $\Delta_\perp$ in the matrix element has again been replaced by a derivative as in Eq. (A6). Parity invariance Eq. (84) now requires that the partial waves are

odd, $l = 1, 3, 5, \ldots$, and the sum becomes

$$\sum_{l=2}^{\infty}[\ldots] \to \sum_{l=3,5\ldots}^{\infty}[\ldots]. \tag{A17}$$

The sum now starts with $l = 3$ because the $l = 1$ term is zero by Eq. (A7). The spin part of the single-particle operator can be rewritten as

$$\begin{aligned}\gamma^0\gamma^3\tau^3 i(\boldsymbol{\nabla}\times\boldsymbol{\gamma})^3 &= -\tau^3(\boldsymbol{\Sigma}_\perp\cdot\boldsymbol{\nabla}_\perp),\\ \tau^3 i(\boldsymbol{\nabla}\times\boldsymbol{\gamma})^3 &= -\gamma^0\gamma^5\tau^3 i(\boldsymbol{\nabla}\times\boldsymbol{\Sigma})^3,\end{aligned} \tag{A18}$$

for even and odd k, respectively. Using the grand spin selection rule and Eq. (A18), following the same logic as in the derivation of Eq. (96), the maximum value of l in the sum of Eq. (A16) is now determined as

$$l_{\max}(k) = k+3 \quad (k \text{ even}), \tag{A19a}$$

$$= k+2 \quad (k \text{ odd}). \tag{A19b}$$

In terms of m, the maximum value is given by $l_{\max}(k = m-1)$. Changing the summation variable from l to $l-3$, the maximum value of the new variable is then

$$l_{\max}(m) = m-1 \quad (m \text{ odd}), \tag{A20a}$$

$$= m-2 \quad (m \text{ even}). \tag{A20b}$$

Altogether we obtain the moment of the dipole mean-field GPD $\tilde{G}_{\mathrm{mf},1}$ as

$$\int dx x^{m-1}\tilde{G}_{\mathrm{mf},1}(x,\xi,0) = \sum_{l=0,2,\ldots}^{l_{\max}(m)}\xi^{l+1}\tilde{C}^{ml}_{\mathrm{mf},1}(t=0), \tag{A21}$$

where the generalized mean-field FFs are now given by

$$\begin{aligned}&\tilde{C}^{ml}_{\mathrm{mf},1}(t=0)\\ &= -\frac{N_c}{6M_N^m}\sum_{n,\mathrm{occ}}\sum_{k=0}^{m-1}\binom{m-1}{k}\frac{E_n^{m-1-k}}{2^k}\sum_{j=0}^{k}\binom{k}{j}\\ &\quad\times\langle n|(\gamma^0\gamma^3)^{k+1}\tau^3(\hat{p}^3)^j(\boldsymbol{\nabla}\times\boldsymbol{\gamma})^3\\ &\quad\times\left[\frac{(-2iM_N|\hat{\boldsymbol{x}}|)^{l+3}}{(l+3)!}P_{l+3}\left(\frac{\hat{x}^3}{|\hat{\boldsymbol{x}}|}\right)\right](\hat{p}^3)^{k-j}|n\rangle.\end{aligned} \tag{A22}$$

Equation (A21) shows that the moments of the dipole mean-field GPD $\tilde{G}_{\mathrm{mf},1}$ are odd polynomials in ξ, with a degree given by Eq. (A20). This agrees with the polynomiality properties required by the identification of the mean-field GPD with the conventional GPDs, Eqs. (5) and (63). In particular, the highest power of ξ in the mean-field GPD $\tilde{G}_{\mathrm{mf},1}$ correctly accounts for the fact that its expression in terms of the conventional GPDs in Eq. (63) contains an "extra" power of ξ in the ξE_T^{u-d} term.

3. Quadrupole GPD

The m-th moment of the quadrupole mean-field GPD $G_{\mathrm{mf},2}$ in Eq. (70) is obtained as

$$\begin{aligned}&\int dx x^{m-1}G_{\mathrm{mf},2}(x,\xi,t)\\ &= -\frac{8}{3}\frac{M_N^3N_c}{M_N^m|\boldsymbol{\Delta}_\perp|^2}\sum_{n,\mathrm{occ}}\\ &\quad\times\sum_{k=0}^{m-1}\binom{m-1}{k}\frac{E_n^{m-1-k}}{2^k}\sum_{j=0}^{k}\binom{k}{j}\\ &\quad\times\langle n|(1+\gamma^0\gamma^3)i\epsilon^{3ia}\gamma^i\tau^b(\hat{p}^3)^jX_2^{ab}e^{i\boldsymbol{\Delta}\cdot\hat{\boldsymbol{x}}}(\hat{p}^3)^{k-j}|n\rangle.\end{aligned} \tag{A23}$$

Under the G_5 transformation the single-particle matrix element transforms as

$$\begin{aligned}&\langle n|(1+\gamma^0\gamma^3)\gamma^i\tau^b(\hat{p}^3)^jX_2^{ab}e^{i\boldsymbol{\Delta}\cdot\hat{\boldsymbol{x}}}(\hat{p}^3)^{k-j}|n\rangle\\ &\quad=\langle n|(\gamma^0\gamma^3)^{k+1}\gamma^i\tau^b(\hat{p}^3)^jX_2^{ab}e^{i\boldsymbol{\Delta}\cdot\hat{\boldsymbol{x}}}(\hat{p}^3)^{k-j}|n\rangle,\end{aligned} \tag{A24}$$

where we use the same notation as in Eqs. (91) and (A15). Performing the partial-wave expansion of the function $e^{i\boldsymbol{\Delta}\cdot\hat{\boldsymbol{x}}}$ in Eq. (A24), including the factor $1/|\boldsymbol{\Delta}_\perp|^2$, and taking the limit $t\to 0$, we obtain

$$\begin{aligned}&\lim_{t\to 0,\,\xi\neq 0}-\sum_{l=4}^{\infty}\left(\delta^{ac}\delta^{db}-\frac{1}{2}\delta^{cd}\delta^{ab}\right)\\ &\quad\times\langle n|(\gamma^0\gamma^3)^{k+1}\gamma^i i\epsilon^{3ia}\tau^b(\hat{p}^3)^j\nabla_\perp^c\nabla_\perp^d\\ &\quad\times\left[\frac{(-2i\xi M_N|\hat{\boldsymbol{x}}|)^l}{(2\xi M_N)^4 l!}P_l\left(\frac{\hat{x}^3}{|\hat{\boldsymbol{x}}|}\right)\right](\hat{p}^3)^{k-j}|n\rangle.\end{aligned} \tag{A25}$$

Here we use the relation Eq. (A4), and $X_2^{ab}e^{i\boldsymbol{\Delta}\cdot\hat{\boldsymbol{x}}}$ in Eq. (A24) has been rewritten in terms of the momentum operator:

$$|\boldsymbol{\Delta}_\perp|^2X_2^{ab}e^{i\boldsymbol{\Delta}\cdot\hat{\boldsymbol{x}}} = \left(\delta^{ac}\delta^{bd}-\frac{1}{2}\delta^{cd}\delta^{ab}\right)[\hat{p}_\perp^c\hat{p}_\perp^d, e^{i\boldsymbol{\Delta}\cdot\hat{\boldsymbol{x}}}]. \tag{A26}$$

This expression is the same as the derivative acting on $e^{i\boldsymbol{\Delta}\cdot\hat{\boldsymbol{x}}}$, i.e.,

$$\begin{aligned}&\lim_{t\to 0,\,\xi\neq 0}|\boldsymbol{\Delta}_\perp|^2X_2^{ab}e^{i\boldsymbol{\Delta}\cdot\hat{\boldsymbol{x}}}\\ &\quad=-\sum_{l=4}^{\infty}\left(\delta^{ac}\delta^{bd}-\frac{1}{2}\delta^{cd}\delta^{ab}\right)\\ &\quad\times\nabla_\perp^c\nabla_\perp^d\left[\frac{(-2i\xi M_N|\hat{\boldsymbol{x}}|)^l}{l!}P_l\left(\frac{\hat{x}^3}{|\hat{\boldsymbol{x}}|}\right)\right].\end{aligned} \tag{A27}$$

Note that the lower limit starts from $l=4$ because

$$\left[\left(\delta^{ac}\delta^{db}-\frac{1}{2}\delta^{cd}\delta^{ab}\right)\hat{p}_\perp^c\hat{p}_\perp^d,|\hat{\boldsymbol{x}}|^l P_l\left(\frac{\hat{x}^3}{|\hat{\boldsymbol{x}}|}\right)\right]=0, \tag{A28}$$

for $l=1\ldots3$. Due to the parity transformation given in Eq. (84), the allowed partial waves in Eq. (A25) are even, i.e., $l=4,6,\ldots$. Thus, Eq. (A25) becomes

$$\sum_{l=4}^{\infty}[\ldots]\to\sum_{l=4,6,\ldots}^{\infty}[\ldots]. \tag{A29}$$

In order to apply the grand spin selection rule we convert the 2D irreducible tensors in the single-particle operator into 3D irreducible tensors. The spin part of the operator is rewritten as

$$\begin{aligned}&\gamma^0\gamma^3\gamma^i i\epsilon^{3ia}\tau^b\left(\nabla_\perp^a\nabla_\perp^b-\frac{1}{2}\boldsymbol{\nabla}_\perp^2\delta^{ab}\right)\\&=\left(\nabla^a\nabla^b-\frac{1}{3}\boldsymbol{\nabla}^2\delta^{ab}\right)(\Sigma_\perp^a\tau_\perp^b)\\&\quad+\frac{1}{2}\left(\nabla^3\nabla^3-\frac{1}{3}\boldsymbol{\nabla}^2\right)(\boldsymbol{\Sigma}_\perp\cdot\boldsymbol{\tau}_\perp)\end{aligned} \tag{A30}$$

for even k, and

$$\begin{aligned}&\gamma^i i\epsilon^{3ia}\tau^b\left(\nabla_\perp^a\nabla_\perp^b-\frac{1}{2}\boldsymbol{\nabla}_\perp^2\delta^{ab}\right)\\&=i\gamma^0\gamma^5(\boldsymbol{\nabla}\times\boldsymbol{\Sigma})^3(\boldsymbol{\nabla}_\perp\cdot\boldsymbol{\tau}_\perp)\\&\quad+\frac{1}{2}i\gamma^0\gamma^5(\boldsymbol{\Sigma}\times\boldsymbol{\tau})^3\boldsymbol{\nabla}_\perp^2\end{aligned} \tag{A31}$$

for odd k. Using the grand spin selection rule and Eqs. (A30) and (A31), similar to the logic presented in the derivation of Eq. (96), the maximum value of l is determined as

$$l_{\max}(k)=k+4\quad(k\text{ even}), \tag{A32a}$$

$$=k+3\quad(k\text{ odd}). \tag{A32b}$$

In terms of m, the maximum value is given by $l_{\max}(k=m-1)$. Changing the summation variable from l to $l-4$, the maximum value is then given by

$$l_{\max}(m)=m-1\quad(m\text{ odd}), \tag{A33a}$$

$$=m-2\quad(m\text{ even}). \tag{A33b}$$

Altogether we obtain the moment of the mean-field GPD Eq. (A23) as

$$\int dx x^{m-1}G_{\mathrm{mf},2}(x,\xi,0)=\sum_{l=0,2\ldots}^{l_{\max}(m)}\xi^l C_{\mathrm{mf},2}^{ml}(t=0), \tag{A34}$$

where the generalized mean-field FFs are given by

$$\begin{aligned}C_{\mathrm{mf},2}^{ml}(t=0)=&\frac{N_c}{6M_N^{m-1}}\sum_{n,\mathrm{occ}}\\&\times\sum_{k=0}^{m-1}\binom{m-1}{k}\frac{E_n^{m-1-k}}{2^k}\sum_{j=0}^{k}\binom{k}{j}i\epsilon^{3ia}\\&\times\langle n|(\gamma^0\gamma^3)^{k+1}\gamma^i\tau^b(\hat{p}^3)^j\left(\nabla_\perp^a\nabla_\perp^b-\frac{1}{2}\boldsymbol{\nabla}_\perp^2\delta^{ab}\right)\\&\times\left[\frac{(-2iM_N|\hat{\boldsymbol{x}}|)^{l+4}}{(l+4)!}P_{l+4}\left(\frac{\hat{x}^3}{|\hat{\boldsymbol{x}}|}\right)\right](\hat{p}^3)^{k-j}|n\rangle.\end{aligned} \tag{A35}$$

Equation (A34) shows that the moments of the quadrupole mean-field GPD $\tilde{G}_{\mathrm{mf},2}$ are even polynomials in ξ, with a degree given by Eq. (A33). This agrees with the polynomiality properties required by the identification of the mean-field GPD with the conventional GPDs, Eqs. (5) and (63).

APPENDIX B: SUM RULES OF MULTIPOLE GPDs

1. ξ-even dipole GPD

In this appendix we prove the sum rules for the higher-multipole chiral-odd GPDs in the large-N_c limit. As in Sec. VI, compute the first moment of the mean-field GPDs in the first-quantized representation of Eq. (70), convert it to a spherically symmetric form using the mean-field symmetry, and compare it with the mean-field expression of the tensor FFs. For simplicity we take $t=0$ in the analysis of the sum rules of the higher multipole GPDs; the extension to finite t is straightforward.

The first moment of the ξ-even dipole GPD Eq. (A12) is obtained as

$$\int dx G_{\mathrm{mf},1}(x,\xi,0)=\frac{2}{3}M_N N_c\sum_{n,\mathrm{occ}}\langle n|\gamma^0\gamma^5 i(\boldsymbol{\Sigma}\cdot\hat{\boldsymbol{x}})|n\rangle, \tag{B1}$$

where we have used the relation Eq. (120a) to convert the expression to a rotationally invariant form. Comparing Eq. (B1) with the expression of the anomalous tensor magnetic moment Eq. (117), we verify the sum rule

$$\int dx G_{\mathrm{mf},1}(x,\xi,0)=\kappa_T^{u+d}. \tag{B2}$$

2. ξ-odd dipole GPD

The first moment of the ξ-odd dipole GPDs Eq. (A21) is obtained as

$$\int dx \tilde{G}_{\mathrm{mf},1}(x,\xi,0) = -\frac{2}{15} M_N^2 N_c \xi \sum_{n,\mathrm{occ}} \times \langle n|\gamma^0 \left[(\boldsymbol{\Sigma}\cdot\hat{\boldsymbol{x}})(\boldsymbol{\tau}\cdot\hat{\boldsymbol{x}}) - \frac{1}{3}(\boldsymbol{\Sigma}\cdot\boldsymbol{\tau})\hat{\boldsymbol{x}}^2 \right] |n\rangle, \tag{B3}$$

where we have employed the relation

$$Y_2^{3b}\tau^3\Sigma_\perp^b = \frac{1}{5} Y_2^{ab}\tau^a\Sigma^b + \cdots, \tag{B4}$$

to convert the expression to a rotationally invariant form; the ellipsis denotes structures with t-channel grand spin > 0. Comparing Eq. (B3) with the expression of the tensor quadrupole moment Eq. (117), we verify the sum rule

$$\int dx \tilde{G}_{\mathrm{mf},1}(x,\xi,t) = -\xi E_T^{u-d}(0). \tag{B5}$$

Similar to the case of the monopole GPD in Sec. VI, we obtain the proper ξ dependence of the moment, corresponding to the nonzero moment of ξE_T^{u-d} and the vanishing moment of $\tilde{E}_T^{u-d}$ in Eq. (63).

3. Quadrupole GPD

The first moment of the quadrupole GPDs Eq. (A34) is evaluated using the relation Eq. (A27),

$$\int dx G_{\mathrm{mf},2}(x,\xi,0) = \frac{M_N^2 N_c}{9} \sum_{n,\mathrm{occ}} \langle n|\gamma^0\gamma^3\gamma^i i\epsilon^{3ia} \times \tau^b \left(\nabla_\perp^a \nabla_\perp^b - \frac{1}{2}\nabla_\perp^2 \delta^{ab} \right) \times \left[|\hat{\boldsymbol{x}}|^4 P_4\left(\frac{\hat{x}^3}{|\hat{\boldsymbol{x}}|} \right) \right] |n\rangle. \tag{B6}$$

Applying the derivatives to the expression in brackets, we obtain

$$\int dx G_{\mathrm{mf},2}(x,\xi,0) = \frac{M_N^2 N_c}{3} \sum_{n,\mathrm{occ}} \langle n| \left[Y_2^{ab}(\Omega_{\hat{\boldsymbol{x}}})\Sigma_\perp^a\tau_\perp^b + \frac{1}{2} Y_2^{33}(\Omega_{\hat{\boldsymbol{x}}})(\boldsymbol{\Sigma}_\perp\cdot\boldsymbol{\tau}_\perp) \right] \hat{\boldsymbol{x}}^2 |n\rangle. \tag{B7}$$

Using now the relation

$$Y_2^{ab}\tau_\perp^a\Sigma_\perp^b = \frac{7}{15} Y_2^{ij}\tau^i\Sigma^j + \cdots, \tag{B8}$$

to convert the expression to a rotationally invariant form, we obtain

$$\int dx G_{\mathrm{mf},2}(x,\xi,0) = \frac{2}{15} M_N^2 N_c \sum_{n,\mathrm{occ}} \times \langle n|\gamma^0 \left[(\boldsymbol{\Sigma}\cdot\hat{\boldsymbol{x}})(\boldsymbol{\tau}\cdot\hat{\boldsymbol{x}}) - \frac{1}{3}(\boldsymbol{\Sigma}\cdot\boldsymbol{\tau})\hat{\boldsymbol{x}}^2 \right] |n\rangle. \tag{B9}$$

Comparing this expression with that of the tensor quadrupole moment, Eq. (117), we verify the sum rule

$$\int dx G_{\mathrm{mf},2}(x,\xi,0) = E_T^{u-d}(0). \tag{B10}$$

[1] K. Goeke, M. V. Polyakov, and M. Vanderhaeghen, Hard exclusive reactions and the structure of hadrons, Prog. Part. Nucl. Phys. **47**, 401 (2001).

[2] M. Diehl, Generalized parton distributions, Phys. Rep. **388**, 41 (2003).

[3] A. V. Belitsky and A. V. Radyushkin, Unraveling hadron structure with generalized parton distributions, Phys. Rep. **418**, 1 (2005).

[4] S. Boffi and B. Pasquini, Generalized parton distributions and the structure of the nucleon, Riv. Nuovo Cimento **30**, 387 (2007).

[5] M. Burkardt, Impact parameter dependent parton distributions and off forward parton distributions for $\zeta \to 0$, Phys. Rev. D **62**, 071503 (2000); **66**, 119903(E) (2002).

[6] M. Burkardt, Impact parameter space interpretation for generalized parton distributions, Int. J. Mod. Phys. A **18**, 173 (2003).

[7] M. Diehl, Generalized parton distributions in impact parameter space, Eur. Phys. J. C **25**, 223 (2002); **31**, 277(E) (2003).

[8] E. Leader and C. Lorcé, The angular momentum controversy: What's it all about and does it matter?, Phys. Rep. **541**, 163 (2014).

[9] M. V. Polyakov and P. Schweitzer, Forces inside hadrons: Pressure, surface tension, mechanical radius, and all that, Int. J. Mod. Phys. A **33**, 1830025 (2018).

[10] C. Lorcé, H. Moutarde, and A. P. Trawiński, Revisiting the mechanical properties of the nucleon, Eur. Phys. J. C **79**, 89 (2019).

[11] V. D. Burkert, L. Elouadrhiri, F. X. Girod, C. Lorcé, P. Schweitzer, and P. E. Shanahan, Colloquium: Gravitational form factors of the proton, Rev. Mod. Phys. **95**, 041002 (2023).

[12] V. Barone, A. Drago, and P. G. Ratcliffe, Transverse polarisation of quarks in hadrons, Phys. Rep. **359**, 1 (2002).

[13] M. Burkardt, Transverse deformation of parton distributions and transversity decomposition of angular momentum, Phys. Rev. D **72**, 094020 (2005).

[14] M. Diehl and P. Hagler, Spin densities in the transverse plane and generalized transversity distributions, Eur. Phys. J. C **44**, 87 (2005).

[15] S. Ahmad, G. R. Goldstein, and S. Liuti, Nucleon tensor charge from exclusive π^0 electroproduction, Phys. Rev. D **79**, 054014 (2009).

[16] S. V. Goloskokov and P. Kroll, An attempt to understand exclusive π^+ electroproduction, Eur. Phys. J. C **65**, 137 (2010).

[17] S. V. Goloskokov and P. Kroll, Transversity in hard exclusive electroproduction of pseudoscalar mesons, Eur. Phys. J. A **47**, 112 (2011).

[18] G. R. Goldstein, J. O. Gonzalez Hernandez, and S. Liuti, Easy as π^0: On the interpretation of recent electroproduction results, J. Phys. G **39**, 115001 (2012).

[19] E. Fuchey *et al.*, Exclusive neutral pion electroproduction in the deeply virtual regime, Phys. Rev. C **83**, 025201 (2011).

[20] M. Defurne *et al.* (Jefferson Lab Hall A Collaboration), Rosenbluth separation of the π^0 electroproduction cross section, Phys. Rev. Lett. **117**, 262001 (2016).

[21] M. Mazouz *et al.* (Jefferson Lab Hall A Collaboration), Rosenbluth separation of the π^0 electroproduction cross section off the neutron, Phys. Rev. Lett. **118**, 222002 (2017).

[22] I. Bedlinskiy *et al.* (CLAS Collaboration), Measurement of exclusive π^0 electroproduction structure functions and their relationship to transversity GPDs, Phys. Rev. Lett. **109**, 112001 (2012).

[23] I. Bedlinskiy *et al.* (CLAS Collaboration), Exclusive π^0 electroproduction at $W > 2$ GeV with CLAS, Phys. Rev. C **90**, 025205 (2014); **90**, 039901(E) (2014).

[24] I. Bedlinskiy *et al.* (CLAS Collaboration), Exclusive η electroproduction at $W > 2$ GeV with CLAS and transversity generalized parton distributions, Phys. Rev. C **95**, 035202 (2017).

[25] M. Dlamini *et al.* (Jefferson Lab Hall A Collaboration), Deep exclusive electroproduction of π^0 at high Q^2 in the quark valence regime, Phys. Rev. Lett. **127**, 152301 (2021).

[26] A. Kim *et al.* (CLAS Collaboration), Beam spin asymmetry measurements of deeply virtual π^0 production with CLAS12, Phys. Lett. B **849**, 138459 (2024).

[27] M. G. Alexeev *et al.* (COMPASS Collaboration), Measurement of the cross section for hard exclusive π^0 muoproduction on the proton, Phys. Lett. B **805**, 135454 (2020).

[28] G. D. Alexeev *et al.* (COMPASS Collaboration), Measurement of the hard exclusive π^0 muoproduction cross section at COMPASS, arXiv:2412.19923.

[29] R. Abdul Khalek *et al.*, Science requirements and detector concepts for the electron-ion collider: EIC yellow report, Nucl. Phys. **B1026**, 122447 (2022).

[30] K. Aoki *et al.*, Extension of the J-PARC hadron experimental facility: Third white paper, arXiv:2110.04462.

[31] R. Enberg, B. Pire, and L. Szymanowski, Transversity GPD in photo- and electroproduction of two vector mesons, Eur. Phys. J. C **47**, 87 (2006).

[32] R. Boussarie, B. Pire, L. Szymanowski, and S. Wallon, Exclusive photoproduction of a $\gamma\rho$ pair with a large invariant mass, J. High Energy Phys. 02 (2017) 054; 10 (2018) 29.

[33] G. Duplančić, S. Nabeebaccus, K. Passek-Kumerički, B. Pire, L. Szymanowski, and S. Wallon, Probing chiral-even and chiral-odd leading twist quark generalized parton distributions through the exclusive photoproduction of a $\gamma\rho$ pair, Phys. Rev. D **107**, 094023 (2023).

[34] G. 't Hooft, A planar diagram theory for strong interactions, Nucl. Phys. **B72**, 461 (1974).

[35] E. Witten, Baryons in the $1/N$ expansion, Nucl. Phys. **B160**, 57 (1979).

[36] S. R. Coleman and E. Witten, Chiral-symmetry breakdown in large-N chromodynamics, Phys. Rev. Lett. **45**, 100 (1980).

[37] J.-L. Gervais and B. Sakita, Large-N QCD baryon dynamics: Exact results from its relation to the static strong coupling theory, Phys. Rev. Lett. **52**, 87 (1984).

[38] R. F. Dashen, E. E. Jenkins, and A. V. Manohar, $1/N_c$ expansion for baryons, Phys. Rev. D **49**, 4713 (1994); **51**, 2489(E) (1995).

[39] D. Diakonov, V. Y. Petrov, and P. V. Pobylitsa, A chiral theory of nucleons, Nucl. Phys. **B306**, 809 (1988).

[40] M. Wakamatsu and H. Yoshiki, A chiral quark model of the nucleon, Nucl. Phys. **A524**, 561 (1991).

[41] C. V. Christov, A. Blotz, H.-C. Kim, P. Pobylitsa, T. Watabe, T. Meissner, E. Ruiz Arriola, and K. Goeke, Baryons as nontopological chiral solitons, Prog. Part. Nucl. Phys. **37**, 91 (1996).

[42] P. Schweitzer and C. Weiss, Spin-flavor structure of chiral-odd generalized parton distributions in the large- N_c limit, Phys. Rev. C **94**, 045202 (2016).

[43] M. P. Mattis, The $I(t) = J(t)$ rule in action, Phys. Rev. D **39**, 994 (1989).

[44] M. P. Mattis and M. Mukherjee, The $I(t) = J(t)$ rule: A new large N_c selection rule for meson—baryon scattering, Phys. Rev. Lett. **61**, 1344 (1988).

[45] R. F. Lebed, The large N_c baryon-meson $I(t) = J(t)$ rule holds for three flavors, Phys. Lett. B **639**, 68 (2006).

[46] J. A. Sheikh, J. Dobaczewski, P. Ring, L. M. Robledo, and C. Yannouleas, Symmetry restoration in mean-field approaches, J. Phys. G **48**, 123001 (2021).

[47] K. Goeke, J. Grabis, J. Ossmann, M. V. Polyakov, P. Schweitzer, A. Silva, and D. Urbano, Nucleon form-factors of the energy momentum tensor in the chiral quark-soliton model, Phys. Rev. D **75**, 094021 (2007).

[48] M. Gockeler, P. Hagler, R. Horsley, D. Pleiter, P. E. L. Rakow, A. Schafer, G. Schierholz, and J. M. Zanotti (QCDSF and UKQCD Collaborations), Quark helicity flip generalized parton distributions from two-flavor lattice QCD, Phys. Lett. B **627**, 113 (2005).

[49] M. Göckeler, P. Hägler, R. Horsley, Y. Nakamura, D. Pleiter, P. E. L. Rakow, A. Schäfer, G. Schierholz, H. Stüben, and J. M. Zanotti (QCDSF and UKQCD Collaborations), Transverse spin structure of the nucleon from lattice QCD simulations, Phys. Rev. Lett. **98**, 222001 (2007).

[50] S. Park, R. Gupta, B. Yoon, S. Mondal, T. Bhattacharya, Y.-C. Jang, B. Joó, and F. Winter (Nucleon Matrix Elements (NME) Collaboration), Precision nucleon charges and form factors using $(2+1)$-flavor lattice QCD, Phys. Rev. D **105**, 054505 (2022).
[51] C. Alexandrou, K. Cichy, M. Constantinou, K. Hadjiyiannakou, K. Jansen, A. Scapellato, and F. Steffens, Transversity GPDs of the proton from lattice QCD, Phys. Rev. D **105**, 034501 (2022).
[52] C. Alexandrou *et al.*, Moments of the nucleon transverse quark spin densities using lattice QCD, Phys. Rev. D **107**, 054504 (2023).
[53] P. Hagler, Form-factor decomposition of generalized parton distributions at leading twist, Phys. Lett. B **594**, 164 (2004).
[54] S. J. Brodsky, H.-C. Pauli, and S. S. Pinsky, Quantum chromodynamics and other field theories on the light cone, Phys. Rep. **301**, 299 (1998).
[55] W. Cosyn and C. Weiss, Polarized electron-deuteron deep-inelastic scattering with spectator nucleon tagging, Phys. Rev. C **102**, 065204 (2020).
[56] J.-Y. Kim, B.-D. Sun, D. Fu, and H.-C. Kim, Mechanical structure of a spin-1 particle, Phys. Rev. D **107**, 054007 (2023).
[57] J.-Y. Kim, H.-Y. Won, J. L. Goity, and C. Weiss, QCD angular momentum in $N \to \Delta$ transitions, Phys. Lett. B **844**, 138083 (2023).
[58] J.-Y. Kim, Electromagnetic multipole structure of a spin-one particle: Abel tomography case, Phys. Rev. D **106**, 014022 (2022).
[59] C. Lorcé, Charge distributions of moving nucleons, Phys. Rev. Lett. **125**, 232002 (2020).
[60] E. Witten, Current algebra, baryons, and quark confinement, Nucl. Phys. **B223**, 433 (1983).
[61] V. B. Berestetskii, E. M. Lifshitz, and L. P. Pitaevskii, *Quantum Electrodynamics*, Course of Theoretical Physics Vol. 4 (Pergamon Press, Oxford, 1982).
[62] P. V. Pobylitsa and M. V. Polyakov, New positivity bounds on parton distributions in multicolored QCD, Phys. Rev. D **62**, 097502 (2000).
[63] D. Diakonov, V. Petrov, P. Pobylitsa, M. V. Polyakov, and C. Weiss, Nucleon parton distributions at low normalization point in the large N_c limit, Nucl. Phys. **B480**, 341 (1996).
[64] D. A. Varshalovich, A. N. Moskalev, and V. K. Khersonskii, *Quantum Theory of Angular Momentum: Irreducible Tensors, Spherical Harmonics, Vector Coupling Coefficients, 3nj Symbols* (World Scientific Publishing Company, Singapore, 1988).
[65] K. Tezgin, B. Maynard, and P. Schweitzer, Chiral-odd GPDs in the bag model, Phys. Rev. D **110**, 054028 (2024).
[66] B. Pasquini, M. Pincetti, and S. Boffi, Chiral-odd generalized parton distributions in constituent quark models, Phys. Rev. D **72**, 094029 (2005).
[67] J.-Y. Kim and C. Weiss (to be published).
[68] P. Schweitzer, S. Boffi, and M. Radici, Polynomiality of unpolarized off forward distribution functions and the D term in the chiral quark soliton model, Phys. Rev. D **66**, 114004 (2002).
[69] P. Schweitzer, M. Colli, and S. Boffi, Polynomiality of helicity off forward distribution functions in the chiral quark soliton model, Phys. Rev. D **67**, 114022 (2003).
[70] D. Diakonov, V. Y. Petrov, P. V. Pobylitsa, M. V. Polyakov, and C. Weiss, Unpolarized and polarized quark distributions in the large N_c limit, Phys. Rev. D **56**, 4069 (1997).
[71] L. D. Landau and E. M. Lifshits, *Quantum Mechanics: Non-Relativistic Theory, Course of Theoretical Physics* Vol. 3 (Butterworth-Heinemann, Oxford, 1991).
[72] H.-C. Kim, M. V. Polyakov, and K. Goeke, Nucleon tensor charges in the SU(2) chiral quark-soliton model, Phys. Rev. D **53**, R4715 (1996).
[73] H.-C. Kim, M. V. Polyakov, and K. Goeke, Tensor charges of the nucleon in the SU(3) chiral quark soliton model, Phys. Lett. B **387**, 577 (1996).
[74] T. Ledwig, A. Silva, and H.-C. Kim, Anomalous tensor magnetic moments and form factors of the proton in the self-consistent chiral quark-soliton model, Phys. Rev. D **82**, 054014 (2010).
[75] S. Diehl *et al.*, Exploring baryon resonances with transition generalized parton distributions: status and perspectives, arXiv:2405.15386.
[76] P. Kroll and K. Passek-Kumerički, Transition GPDs and exclusive electroproduction of π-$\Delta(1232)$ final states, Phys. Rev. D **107**, 054009 (2023).
[77] S. Diehl *et al.* (CLAS Collaboration), First measurement of hard exclusive $\pi^-\Delta^{++}$ electroproduction beam-spin asymmetries off the proton, Phys. Rev. Lett. **131**, 021901 (2023).
[78] A. Bhoonah and C. Lorcé, Quark transverse spin–orbit correlations, Phys. Lett. B **774**, 435 (2017).
[79] C. Mezrag, An introductory lecture on generalised parton distributions, Few-Body Syst. **63**, 62 (2022).